FINAL TECHNICAL REPORT

A STUDY OF MICROSTRUCTURAL CHARACTERISTICS OF Ni-BASED SUPERALLOYS AT HIGH TEMPERATURES

Submitted to

NATIONAL AERONAUTICS AND SPACE ADMINISTRATION
WASHINGTON, D.C

Department of Physics

Alabama Agricultural and Mechanical University
P.O. Box 428
Normal, Alabama 35762

December 1990

FINAL TECHNICAL REPORT

ON

NASA GRANT NAG8-076

A Study of Microstructural Characteristics of Ni-Based Superalloys at High Temperatures

Principal Investigator : Ravindra B. Lal
Professor of Physics
Alabama A and M University
Normal, Al 35762
Tel No. (205) 851-5309

Co-Investigator : M.D.Aggarwal
Associate Professor of Physics
Department of Physics
Tel No. (205) 851-5308

Submitted to

National Aeronautics and Space Administration
George C. Marshall Space Flight Center
Marshall Space Flight Center, Al 35812

December, 1990

Report No. AAMU-NAG-003

TABLE OF CONTENTS

PREFACE

The present report dated November 1990 is an interim technical report on NASA Grant NAG8-076 after two years of intermittent funding. The project officially was granted on October 1,1986 and second year renewal was granted February, 1988. A renewal proposal was submitted to NASA on February,1989 and funding is awaited. The work was initiated by modifying our existing experimental facilities to work on superalloys. To initiate the work in a proper direction and plan out our mode of investigation, a meeting was arranged on Oct. 20,1986 with Dr. E.C. McKannan, Dr. Bilyar Bhat, Mr. Richard Parr and Ms Wendy Alter of Materials laboratory of Marshall Space Flight Center. After that, meetings were arranged at various stages of the project. Our last meeting was with the present technical monitor of the project Dr. Stephen Gentz and Mr. Richard Parr.

We thank Mr. Richard Parr for providing us the samples of superalloy rod MAR-M246(Hf) and PWA1480. We also thank Mr. Richard J. Quigg, Vice President of Cannon-Muskegon Corporation for providing us with polycrystalline samples of CMSX-2 and CMSX-3 and Mr. Gregory Bell of Howmet Corporation for providing single crystal specimen of Ni-based superalloy CMSX-2 and CMSX-3. Thanks are also due to Mr. Samuel O. Mancuso of Special Metals Corporation for providing us with the samples of MAR-M247, UD-41 and Waspaloy. Prof. Ye. T. Chou of Lehigh University has been helping us as a consultant

during the progress of the project. Mr. Samuel Oyekenu worked as a graduate student on the project.

Summary

The objective of this investigation is to study the microstructural characteristics of the Ni-based superalloy MAR-M246(Hf) which is used in manufacturing the components of the Space Shuttle's main engine. These superalloys need optimum heat treatment to get the best results. To find out the optimum heat treatment the techniques of differential thermal analysis (DTA) and the optical photomicrographs were utilized. In the first phase, the existing experimental equipment like cutting, grinding/polishing machines and metalllurgical microscope have been set up to cut/polish and take the photomicrographs. In the beginning of the project a Perkin Elmer differential thermal analyzer DTA1700 alongwith temperature programmer and the needed computer interface was procured and made operational. In the second year Leitz Metallux-3 hot stage research microscope has also been procured and installed for in-situ observation of the superalloy samples. The hot stage when tested for the first time alloyed the thermocouple with the Tantalum heating element and has now been installed finally by the supplier.

Samples of MAR-M246(Hf), MAR-M247, Waspaloy, Udimet-41, CMSX-2 and CMSX-3 (polycrystalline and single crystals) have been studied using differential thermal analyzer and the results are reported here. Photomicrographs of the Ni-based

superalloy MAR-M246(Hf) has been recorded before and after heat treatment at certain temperatures. More heat treatments need to be done before a final inference can be arrived at.

1. INTRODUCTION

1.1 Technical Background

Superalloys are an important class of materials and have made much of our very high temperature engineering technology possible.They are complex materials capable of maintaining certain of their room temperature physical and mechanical properties at elevated temperatures. Superalloys can be divided in three broad classes : Nickel base superalloys, cobalt base superalloys and iron base superalloys. Iron generally disappeared as an alloy base in favor of nickel and cobalt since they stabilized the stronger FCC structure. Mechanical properties such as strength, ductility, toughness of metals and alloys are strongly dependent on their type of structure. Hexagonal close packed metals commonly have less strength than the fcc and bcc metals. Because of the packing arrangement, their ductility is more dependent on direction than fcc and bcc metals. Nickel based superalloys have found widespread applications because of their corrosion resistance, high strength and the capability of maintaining their room temperature physical and mechanical properties at elevated temperatures. Essentially a superalloy can be considered as a "chemical stew" containing as much as 14 different elements[1]. Nickel is an ideal base for such alloys because of its high melting point 1453 C (2647F), adequate corrosion resistance and ability to dissolve a number of other metallic elements which serve to strengthen

it. In the present investigation, nickel base superalloy manufactured by Martin Marietta MAR- M246(Hf) has been selected which is used in fabricating components for the space shuttle main engine. This is a directionally solidified material with the weight composition as follows:

Ni	58.035%	Hf	1.75%
Co	10%	Ti	1.5%
W	10%	Ta	1.5%
Cr	9%	C	0.15%
Al	5.5%	Zr	0.05%
Mo	2.5%	B	0.015%

The different elements go into the solid solution to provide one or more of the following effects:

Strength	Mo,Ta,W
Oxidation Resistance	Cr, Al
Phase Stability	Ni
Gamma Prime	Al, Ti

The γ' phase is the key factor responsible for the extraordinary useful high temperature properties of Ni-based superalloys and has a complex ordered structure which precipitates coherently with the matrix to provide precipitate hardening. The major phases present in the microstructure of these nickel superalloys[1] are gamma matrix (γ) the intermetallic precipitate gamma prime (γ'), carbides like MC, $M_{23}C_6$ and M_6C. M_6C and $M_{23}C_6$ tend to populate the

grain boundaries. In addition, constituents such as sigma (σ), mu (μ) and Laves phases are found in Ni based superalloys.

The observation of polished and etched samples under an optical microscope is one of the most useful and easily applied technique for establishing the microstructure of superalloys. However, as with any visual technique it depends critically upon the sampling procedure selected since the region viewed represents only a small fraction of the total volume of the material. Since sample selection is such an important stage in any microstructural evaluation it must be undertaken to ensure that all necessary and appropriate information will be observed. Indeed it is often desirable to select samples not only from different regions of the whole but also at various angles. Samples are prepared by a mechanical lapping sequence followed, in certain special circumstances, by final chemical polishing to remove the "flowed" surface layer.

1.2 Objectives of the Project

1. To determine the heat treatment/annealing recipe for the superalloy MAR-M246(Hf) to improve its high temperature performance.

2. To correlate the mechanical properties of Ni-based superalloy MAR-M246(Hf) with structure by systematic study of optical photomicrographs and DTA curves on various heat treated samples.

3. To study other superalloys and compare its behaviour with Ni-based superalloy MAR-M246(Hf).

2. EXPERIMENTAL TECHNIQUES

2.1 Sample Preparation

Ni-based superalloy MAR-M246(Hf) samples were provided by Mr. Richard Parr of Marshall Space Flight Center, Huntsville. Samples of other Ni-superalloys viz., MAR-M247, Waspaloy and Udimet (UD-41) were provided by Mr. Samuel O. Mancuso of Special Metals and polycrystalline samples were provided by Mr. Richard J. Quigg of Cannon-Muskegon corporation and single crystal specimen were supplied by Mr. Gregory Bell of Howmet Corporation.

Samples of MAR-M246(Hf) were cut using low speed diamond saw which took 3 to 4 hours to cut a 3/8 inch diameter rod of the directionally solidified material. The purpose of cutting is to reduce the specimen to a manageable size and to reach the desired plane for observation. The samples were cut parallel, perpendicular and at 45 degree angle to the major axis of the rod. The samples need to have a highly polished surface to reveal the microstructure. To accomplish this, these samples were then embedded in the cold mold using Buehler Castoglass resin and hardener as well as in hot mold which provides a means of holding the specimen during preparation. The cold mold can be dissolved in "Stripsolve" to take the sample out of the mold for later heat treatment or other processing. Pictures of some of the samples in the mold are shown in Figs 1 to 2. Fine grinding reduces the

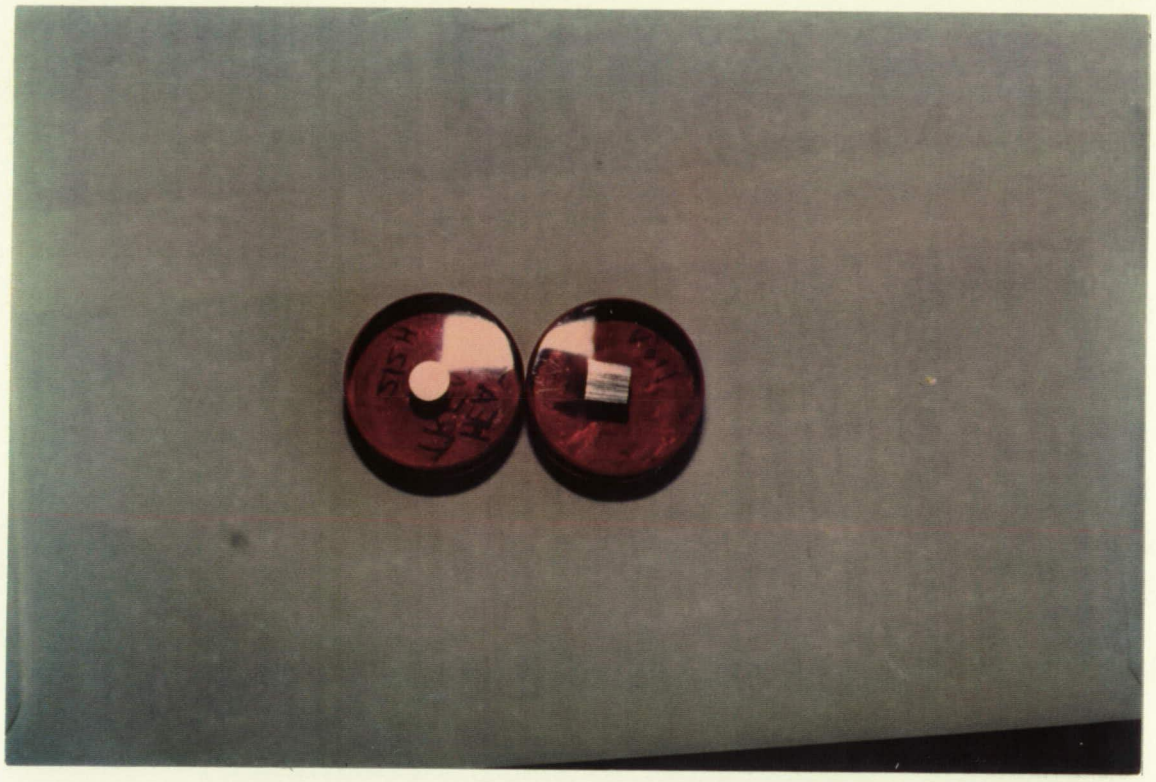

Fig. 1 Ni-based Superalloy MAR-M246(Hf) in Buehler Castoglass and resin molds. Samples # 212H and 110V

Fig.2 Ni-based superalloy MAR-M246(Hf) in the hot and cold molds

deformation level of the specimen surface, preparatory to rough and final polishing. The specimen is grinded on a series of abrasive papers usually 240,320,400 and 600 grit lubricated with water.

Fine grinding is accomplished by using a motor driven polisher/grinder. Rough and final polishing are critical steps, which more than any other steps, determine the success or failure of specimen preparation. Rough polishing is performed on a low nap cloth that has been charged with 6 micron Metadi polishing compound. This step is important because it must remove the fine grinding scratches while maintaining a flat surface. In Ni-based superalloys, samples are prone to deformation during abrasive preparation and these deformation layers tend to obscure incompletely removed grinding scratches. These scratches have a way of reappearing when the finished polished specimens are etched to reveal the microstructure. The best way to avoid this problem is to perform each step thoroughly as though it was the most important one[2,3].

Final cloth polishing is usually performed with 1 micron, 0.3 micron and .05 micron alumina on different microcloths respectively. The purpose of this step is to remove the final traces of scratches and provide the highly polished surface needed to reveal the microstructure.

2.2 Microstructure Development

To prepare the samples for revealing the microstructures, samples are etched using various etchants. It was found better to etch lightly at first, then remove the first light etch by returning briefly to the final polishing step. By polishing off the first etch applied, then reetching, any remaining fine residual scratches are usually removed. The second etch produces sharper, well defined microstructural detail. The etchants which are used are listed below:

1. Kalling's Reagent # 1
   - 5g $CuCl_2$
   - 100 ml Hydrochloric Acid
   - 100 ml Ethanol
   - 40 ml Distilled water

2. Kalling's Reagent
   - 5g $CuCl_2$
   - 100 ml Hydrochloric Acid
   - 100 ml Ethanol

3. Etchant for Gamma prime
   - 50 ml Hydrochloric Acid
   - 1-2 ml H_2O_2(30%)

4. Carbides	100 ml Ethanol 1-3 ml Selenic Acid 20-30 ml Hydrochloric Acid

2.3 Photomicrography

When we examine the microstructure of a material we are looking at very small sample of the structure. From this limited view we have tried to understand how the properties of the material relate to the structure. But when we measure the properties of the material, such as tensile strength, hardness, density etc. we use a much larger specimen, so that the measured properties refer to something hundreds or thousands of times larger than our microscopic view. It should not be surprising, therefore, that it is difficult to establish true correlations between properties and microstructure[4].

In the previous year, we had been using the existing Olympus inverted metallurgical microscope model PME with 35 mm camera attachment. This year Leitz Metallux 3 microscope with a heating stage upto 1750 C is being procured for in-situ observation of the phase changes. This instrument will allow us to heat the sample in vacuum or in inert argon atmosphere upto 1750 C. The sample is placed on a heating band made out of tantalum or tungsten which are heated by means of low voltage high current flowing through them. The

heating elements and the interior of the chamber are covered by a radiation protection plate. Only the surface of the sample remain visible through a small observation window.

Olympus microscope has been used for most of this study and the various photomicrographs attached herewith are for MAR-M246(Hf) before and after heat treatment. Various locations show γ', MC, $M_{23}C_6$ on these photographs. The new microscope with hot stage is completely installed and in operational and we have been able to make in situ observation of different phases at high temperature through the microscope.

Photomicrographs are taken using the Leitz metallux-3 microscope using first order red compensator between the polarizer and analyzer on samples of Ni-based superalloy MAR-M246(Hf) after polishing and etching. A sample cut perpendicular to the major axis of the rod is suffixed by an "H" and the sample cut along the major axis is suffixed by an "V". Photomicrographs (Fig Nos. 3 to 6) are shown for sample # 203H before annealing with or without the first order red compensator. Similarly photomicrographs Nos 7 to 10 are shown for sample # 110V with or without first order red compensator.

An annealed/heat treated sample (1220 + 6 C for 2 hours and 871 + 14 C for 8 hours) was cut perpendicular and parallel to the major axis of a 3/8 inch diameter rod of

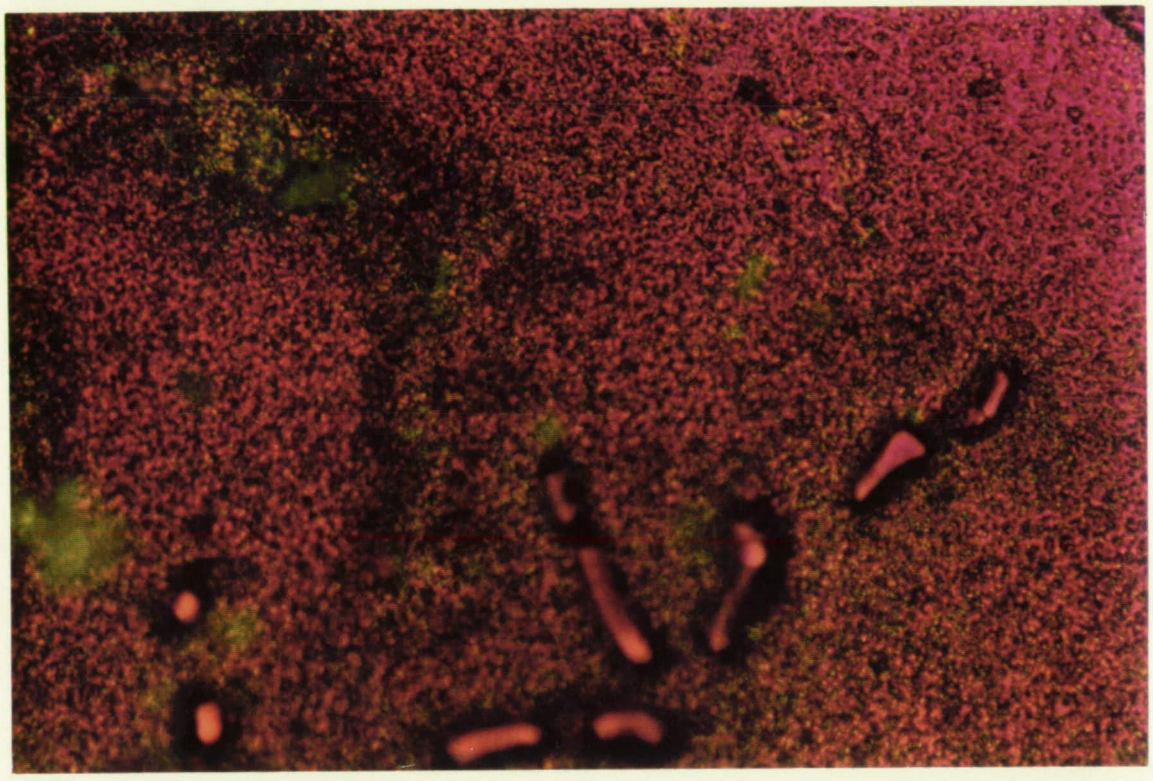

Fig. 3 Photomicrograph of Ni-based Superalloy MAR-M246(Hf) before heat treatment using first order red compensator 667X Sample # 203H

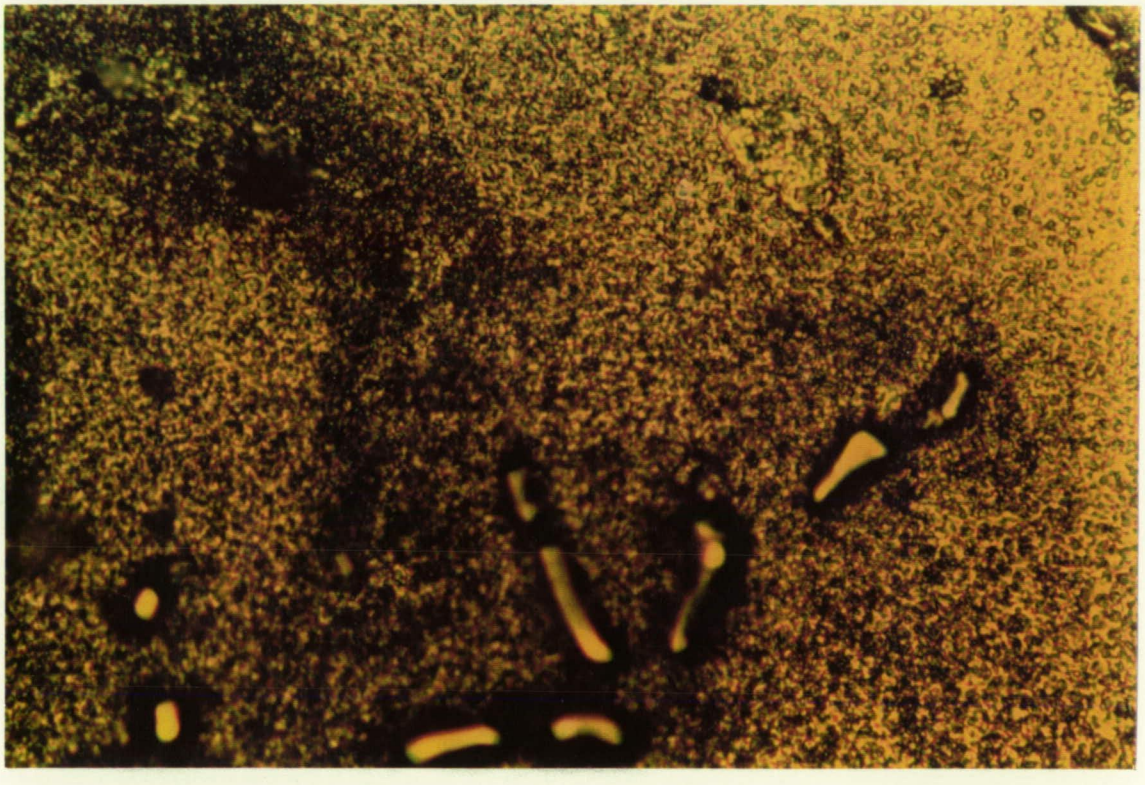

Fig 4 Photomicrograph of Ni-based superalloy MAR-M246(Hf) before heat treatment at 666x (Sample # 203 H)

Fig.5 Photomicrograph of Ni-based superalloy MAR-M246(Hf) before heat treatment (Sample # 203H) using first order red compensator at 666x

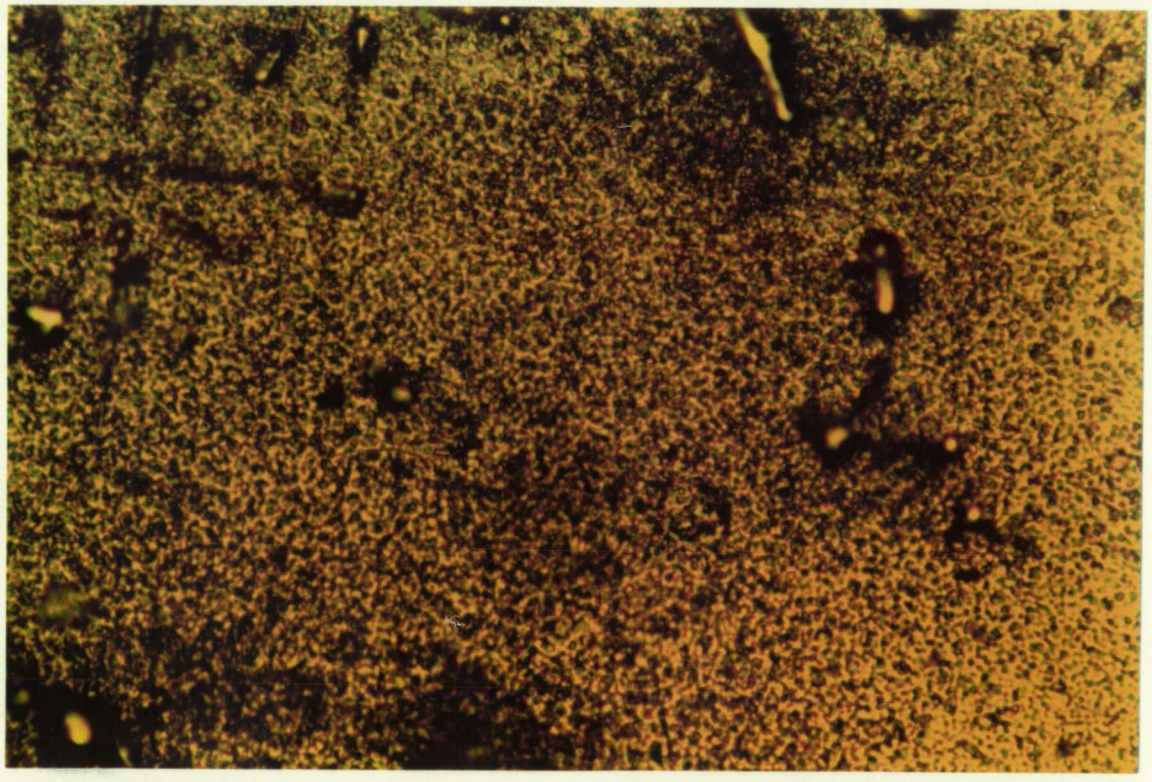

Fig 6 Photomicrograph of Ni-based superalloy MAR-M246(Hf) before heat treatment at 666x (Sample # 203H)

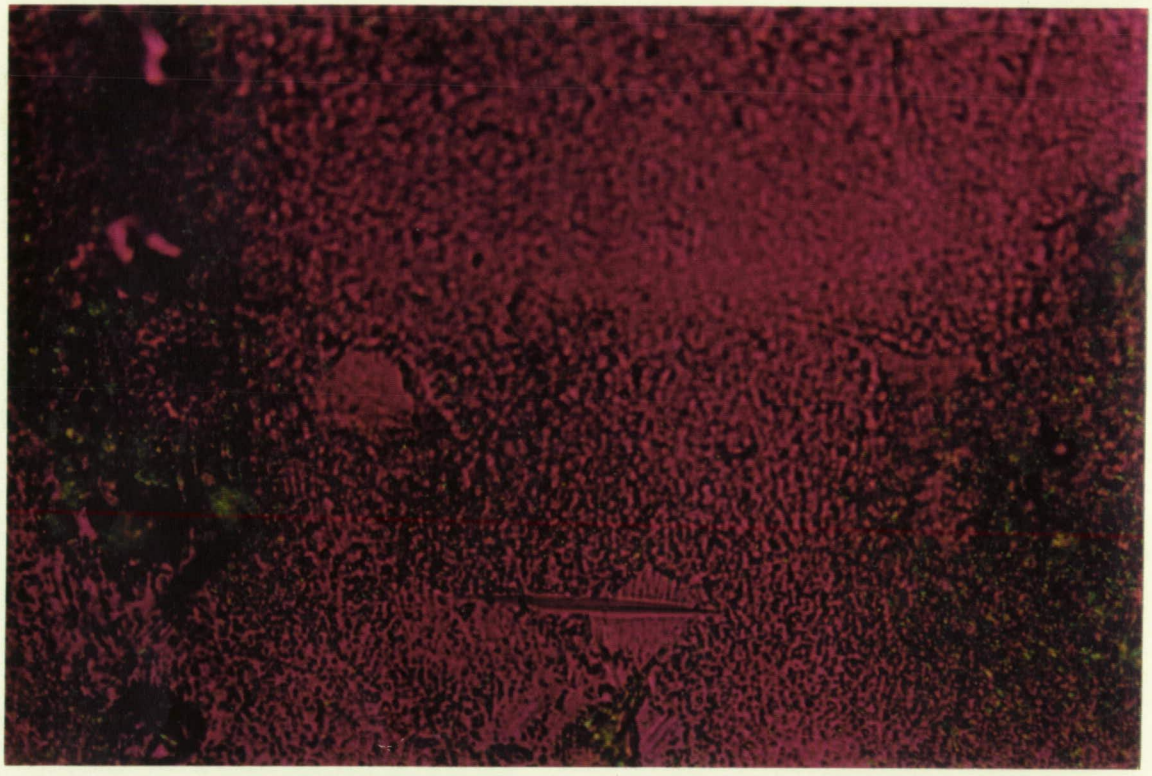

Fig 7 Photomicrograph of Ni-based superalloy MAR-M246(Hf) before heat treatment using first order red compensator Sample # 110 V, 667 X.

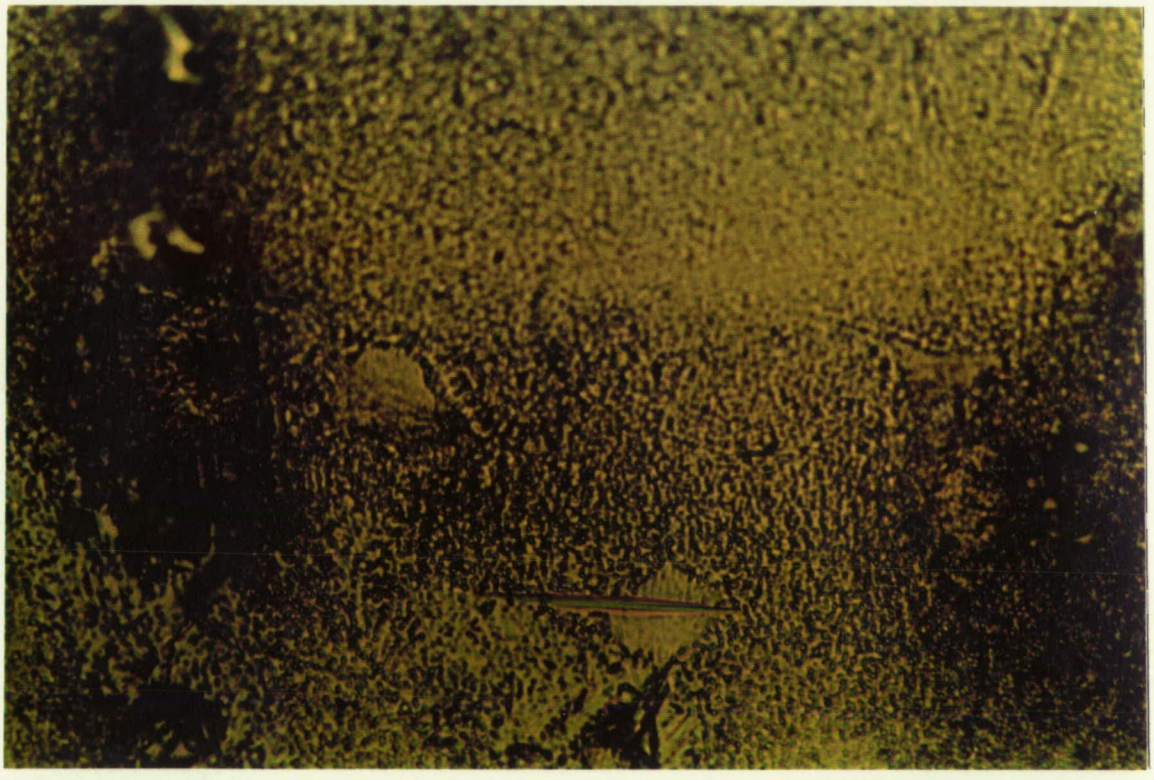

Fig 8 Photomicrograph of Ni-based superalloy MAR-M246(Hf) before heat treatment for Sample # 110V at 667X

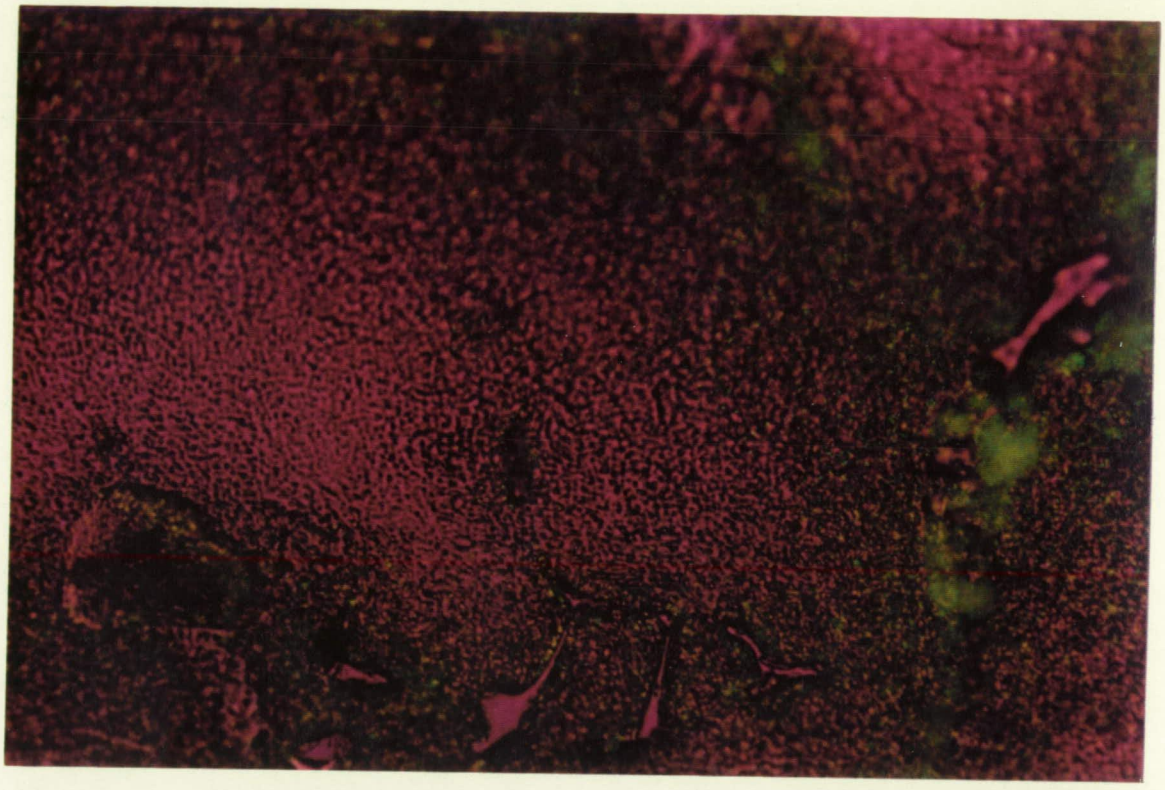

Fig 9 Photomicrograph of Ni-based superalloy MAR-M246(Hf) before annealing using first order red compensator, Sample # 110V at 667X.

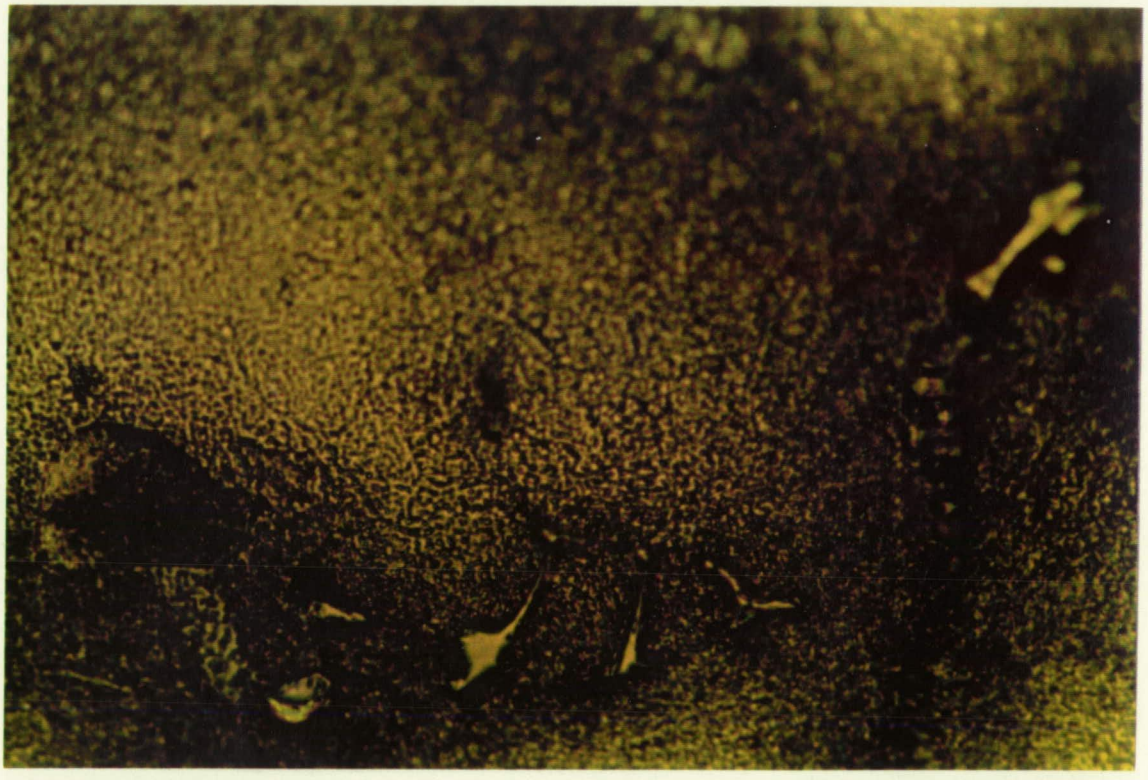

Fig 10 Photomicrograph of Ni-based superalloy MAR-M246(Hf) before annealing for sample # 110V at 667X.

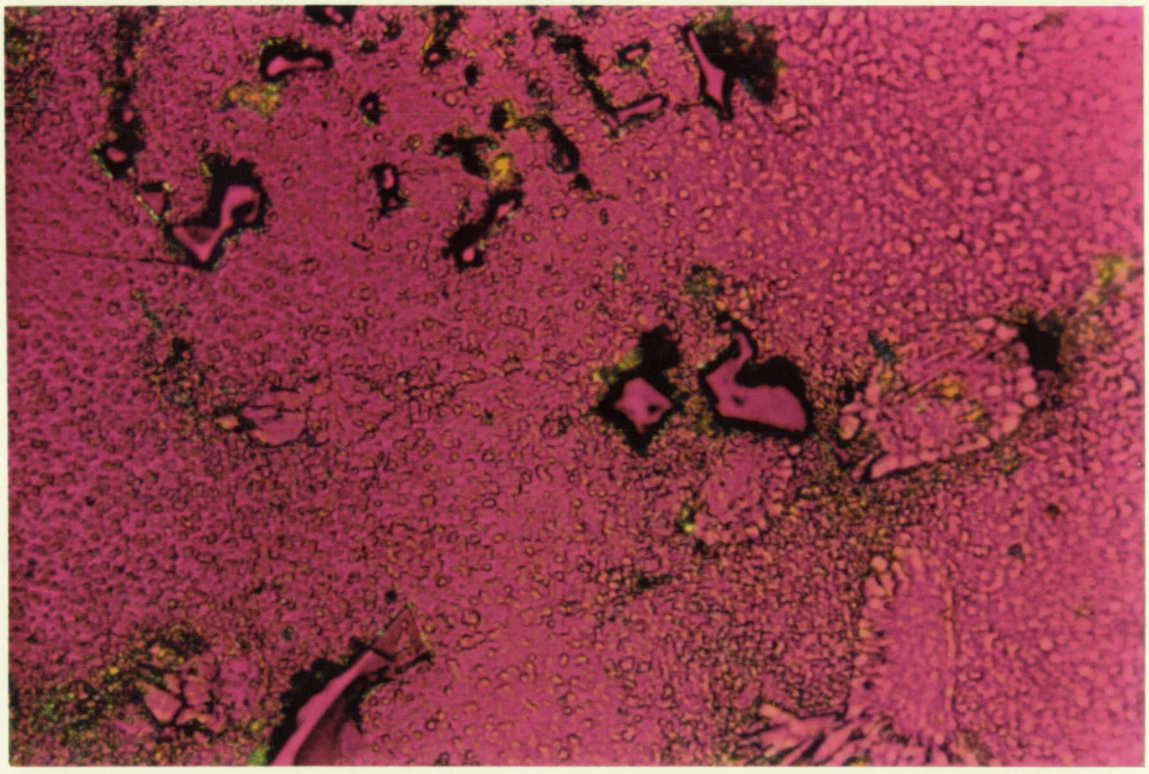

Fig 11. Photomicrograph of Ni-based superalloy MAR-M246(Hf) after heat treatment sample # 212H using red compensator at 667 X

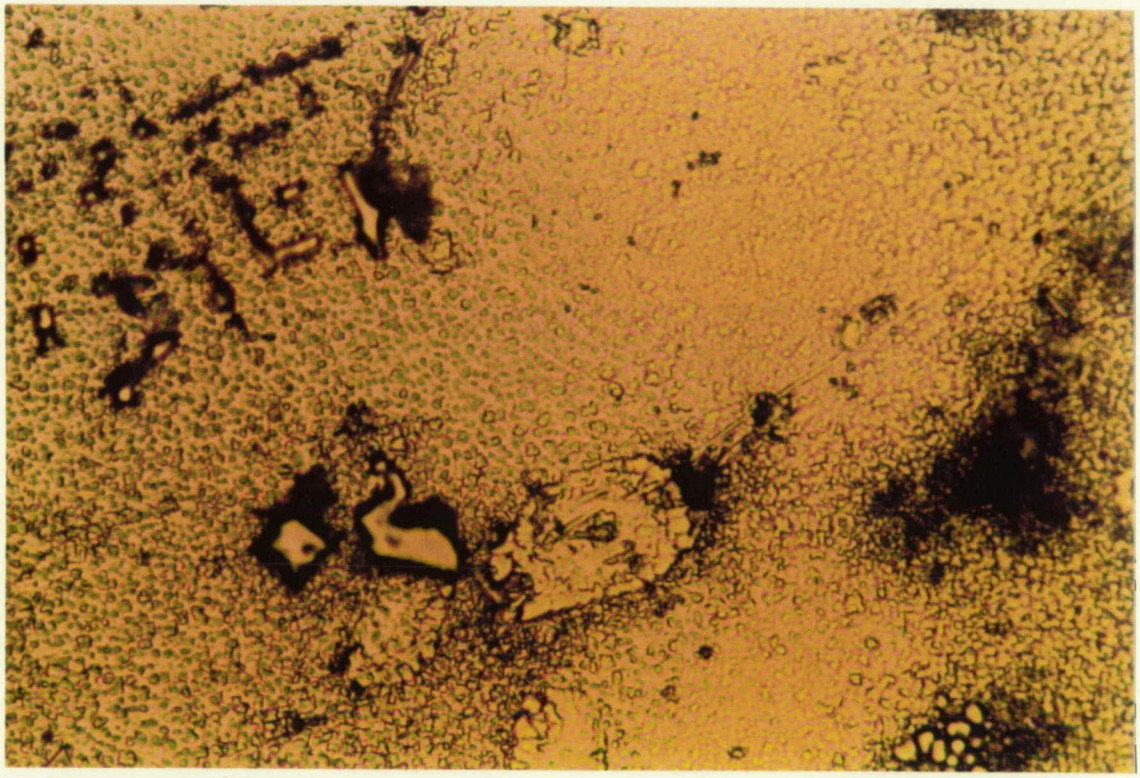

Fig 12 Photomicrograph of Ni-based superalloy MAR-M246(Hf) after heat treatment sample #212H at 667X

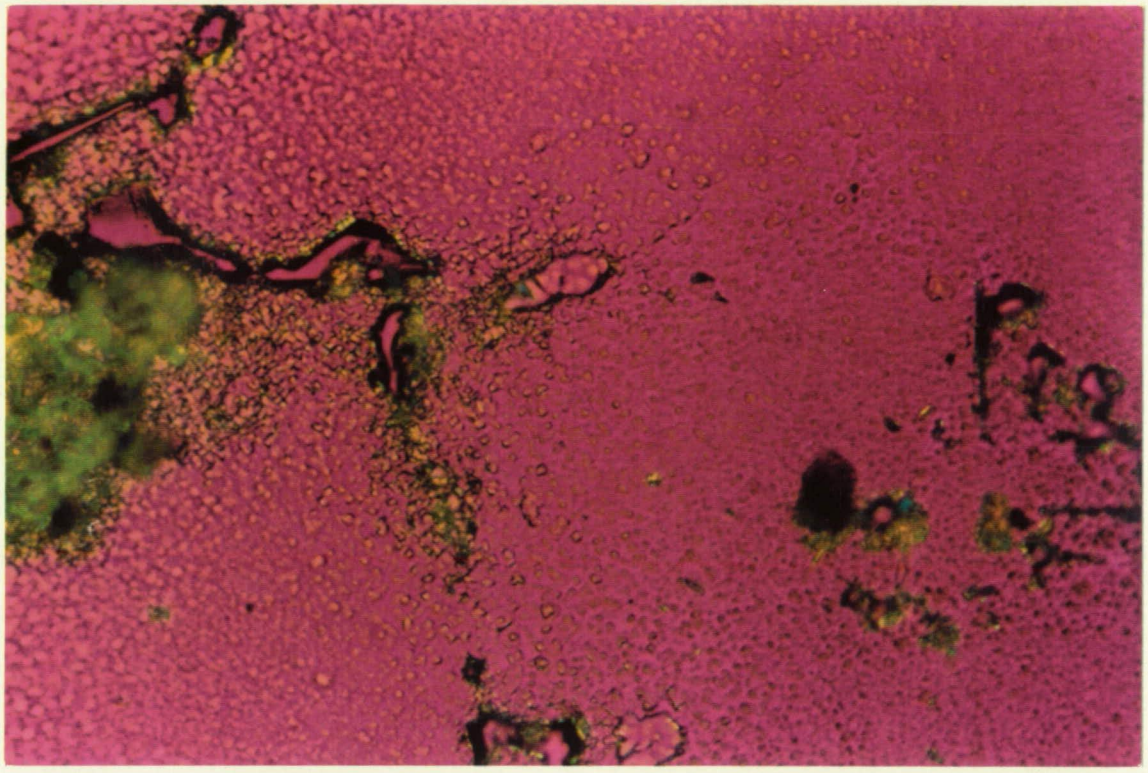

Fig 13 Photomicrograph of Ni-based superalloy MAR-M246(Hf) after heat treatment using red compensator at 667X sample # 212H

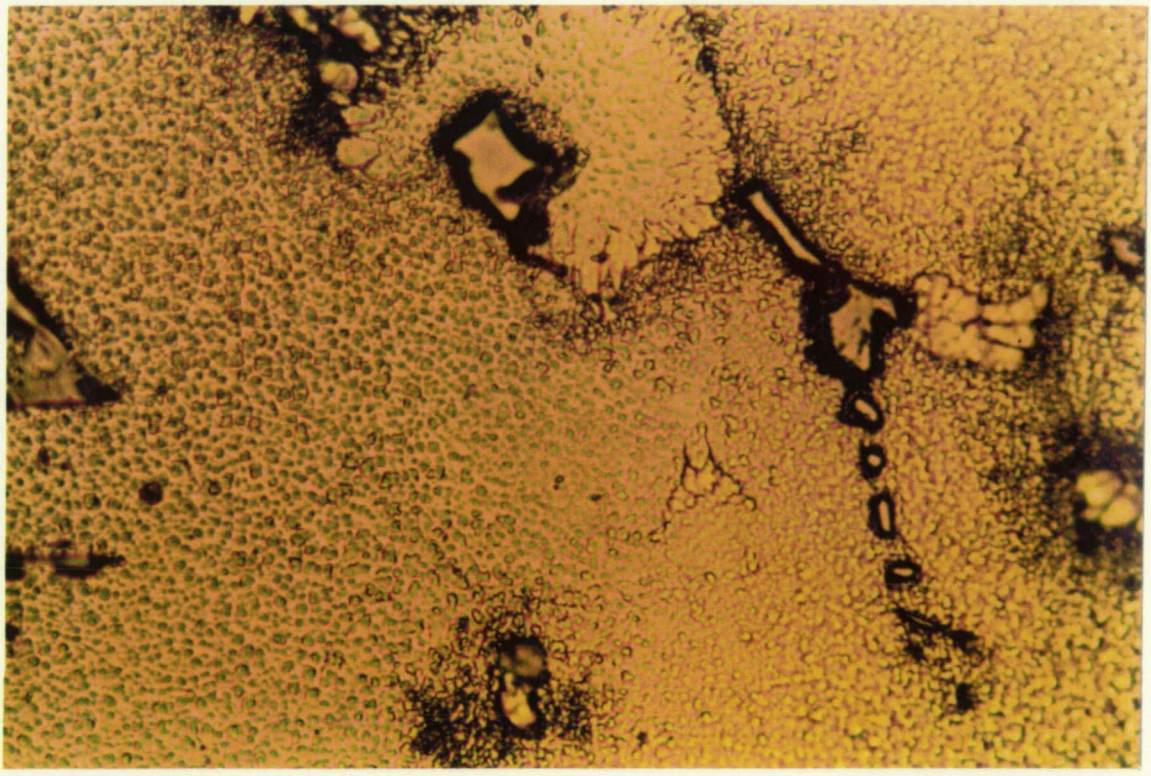

Fig 14 Photomicrograph of Ni-based superalloy MAR-M246(Hf) after heat treatment for sample # 212H at 667X

Fig 15 Photomicrograph of Ni-based superalloy MAR-M246(Hf) after heat treatment for sample # 213V at 667X.

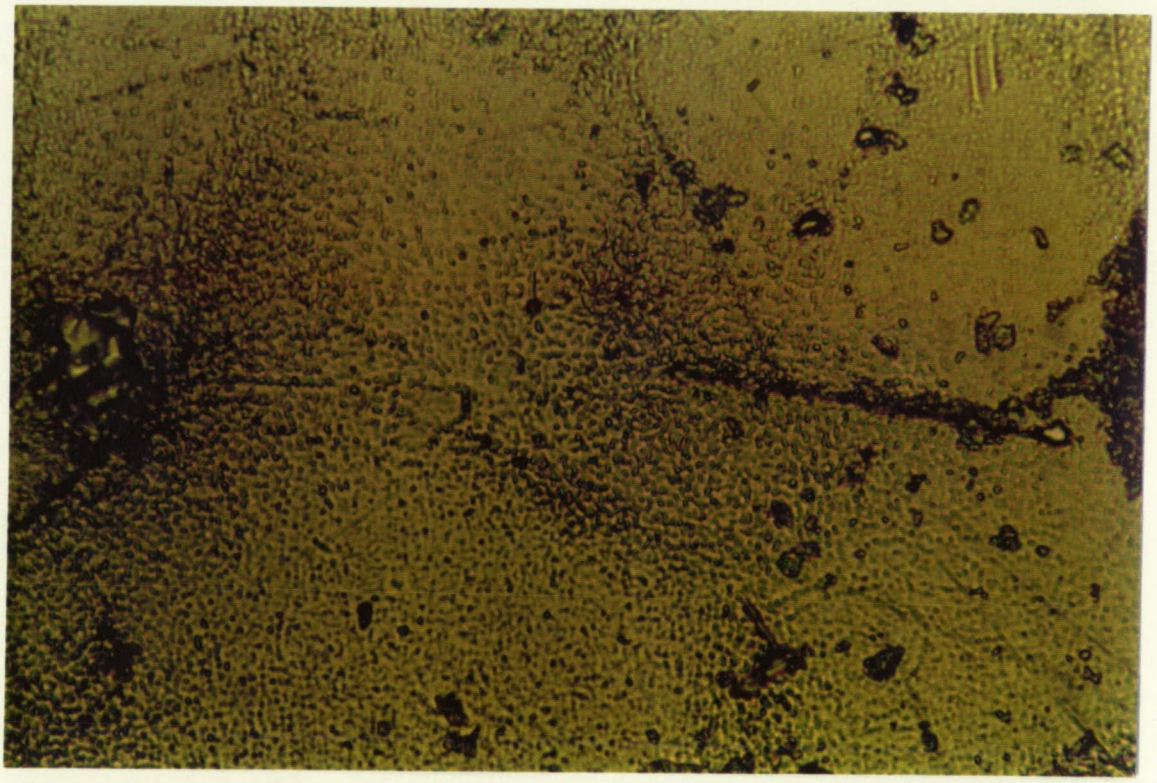

Fig 16 Photomicrograph of Ni-based superalloy MAR-M246(Hf) after heat treatment for sample # 213V at 667X

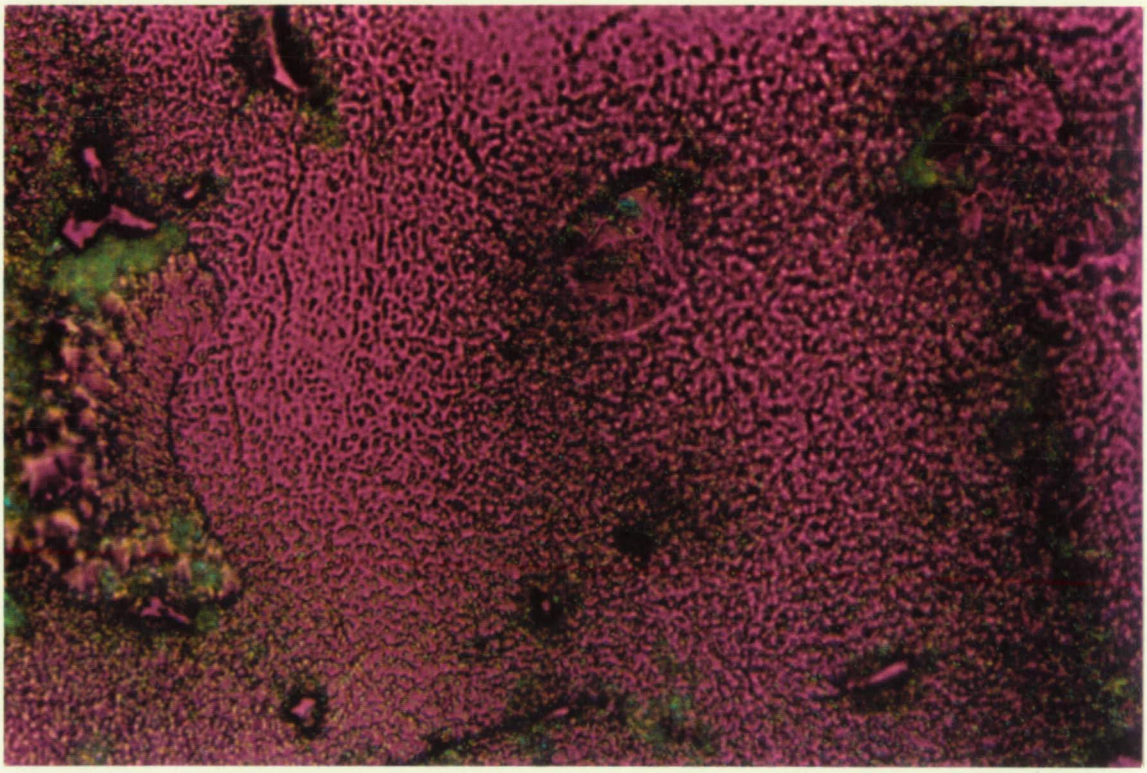

Fig 17 Photomicrograph of Ni-based superalloy MAR-M246(Hf) after heat treatment for sample # 213V at 667X using red compensator.

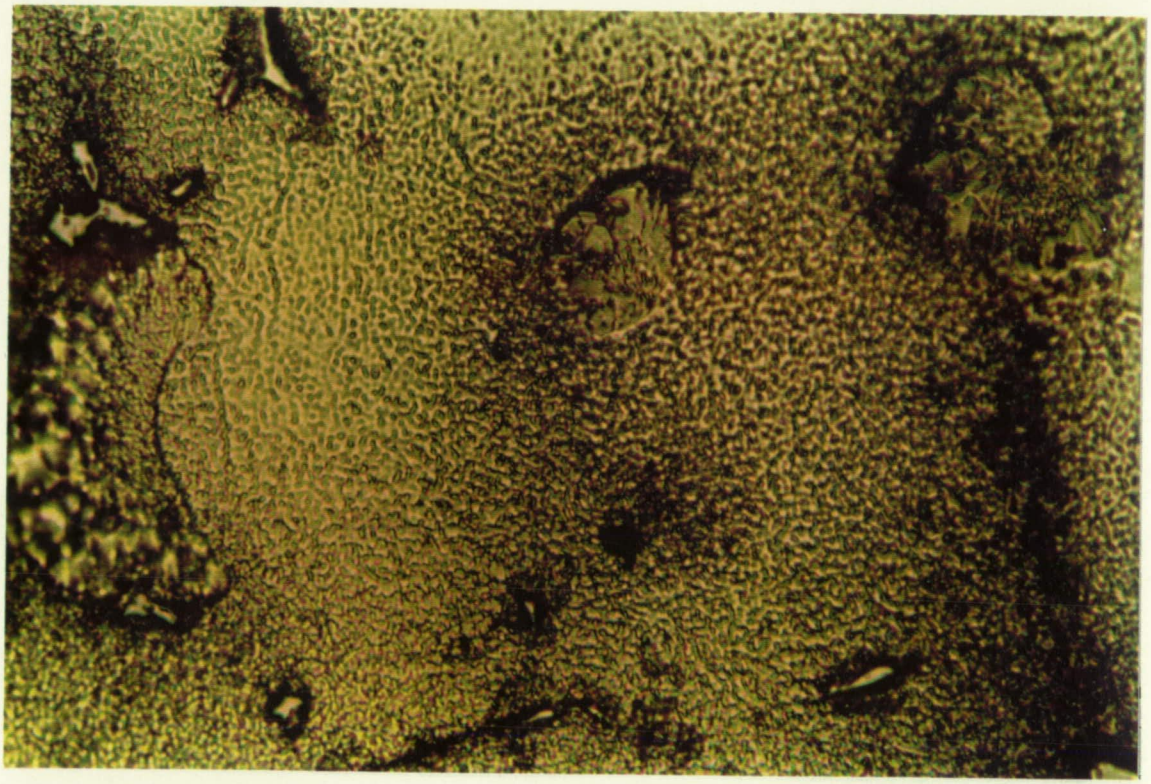

Fig 18 Photomicrograph of Ni-based superalloy MAR-M246(Hf) after heat treatment for sample # 213V at 667X

2.4 Differential Thermal Analysis and Heat Treatment of Superalloys

Differential thermal analysis (DTA) has proved to be a valuable technique for the superalloy metallurgists to study liquidus-solidus data, carbide and boride precipitation reactions, γ' solvus temperatures and incipient melting temperatures. This technique enables accurate determination of the temperatures at which superalloy phase changes occur. It can also be used in the examination of the effects of the variations of alloy designers and casters for insights into solidification phenomena and the general castability of alloys[5].

The technique of differential thermal analysis is in existence for nearly 100 years since its conception by Le Chatelier. It has been traditional that DTA units were built from component parts by the experimenters themselves, the design being dictated by the specific problem. However, in the past 10 years there has been a breakthrough in the commercially available DTA units enabling wide range of application. Because of this, DTA has rapidly become an invaluable tool, not only for alloy design, but for every day metallurgical production, problem solving and quality control.

Superalloys provide a vast field of application of the DTA method. These materials may contain a dozen or more alloying elements and, depending upon the method of

manufacture, heat treatment and service may contain a variety of phases. Phase transitions within a superalloy may occur as a result of chemical reaction or decomposition as well as from melting-freezing or lattice rearrangement. Since DTA is an energy sensitive method,it is uniquely valuable to the determination of high temperature reactions in superalloys.

The transformations of interest in superalloys are of both solid-liquid and solid-solid types. For the case of solid- liquid variety there are solidus and liquidus points, solutioning of carbides and incipient melting. Solid state transformations include carbide, boride and γ' reactions. Knowledge of these rections aids in establishing solutioning and aging heat treatments and cooling procedures.

In the DTA method, a reference sample of similar mass and thermal properties is subjected to the same environment as the measured sample. The reference should exhibit no transformations within the temperature range of interest in order that its heating or cooling rate remain constant.The temperature of the sample and reference are monitored separately and they are also connected in opposite polarity to measure the temperature differential ($\Delta T = T_{sample} - T_{reference}$). ΔT is amplified and then fed to Thermal Analysis Data System which displays a plot of ΔT vs T for any sample. A schematic diagram of the typical DTA apparatus is shown in Fig 19.

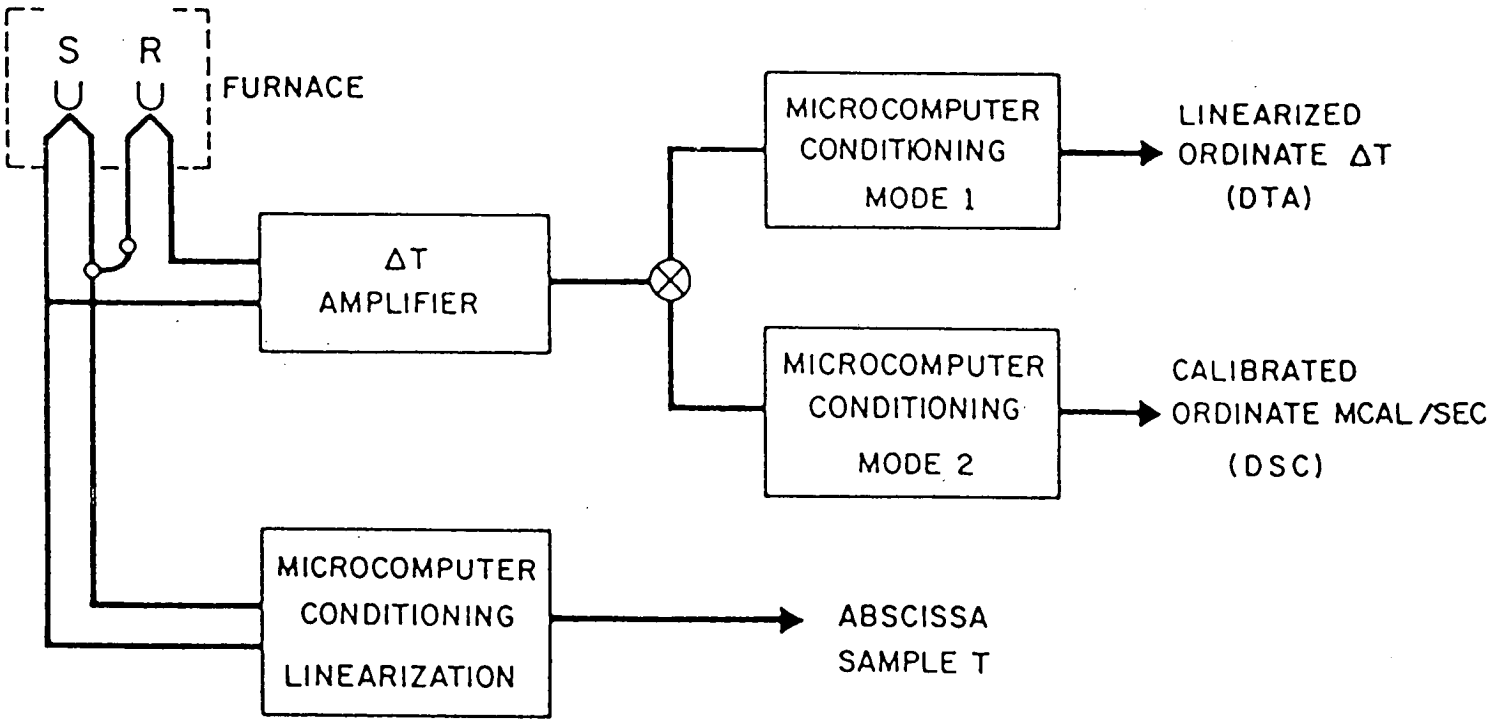
S
R
FURNACE
ΔT
AMPLIFIER
MICROCOMPUTER
CONDITIONING
MODE 1
LINEARIZED
ORDINATE ΔT
(DTA)
MICROCOMPUTER
CONDITIONING
MODE 2
CALIBRATED
ORDINATE MCAL/SEC
(DSC)
MICROCOMPUTER
CONDITIONING
LINEARIZATION
ABSCISSA
SAMPLE T

Fig. 22

It consists of sample holder assembly (incorporating sample and reference containers mounted in a suitable holder, thermocouple etc), furnace, temperature programmer, atmosphere control, cooling control and thermal analysis data station.

As planned, Perkin-Elmer differential thermal analyzer DTA 1700 was procured and installed alongwith thermal analysis data system which was possible only after a trade-in of a component of the existing DSC-4 system purchased under a separate grant. This increased the versatility and usefulness of the equipment.

Fig 20 is a general view of the DTA apparatus, which is a part of the Perkin Elmer DTA 1700 system. External view of the furnace and internal view of the sample holder are shown in Figs 21 and 22. The control thermocouple is Pt/Pt.10%Rh. The unknown sample is always placed in the left side crucible because of the design of the inner circuitry. Silver (melting point : 961 C) and nickel (melting point : 1455 C) are used to caliberate the instrument reasonably near our temperatures of interest. Sample holders/crucibles are made up of high density high purity alumina 6 mm^3 and 10 mm^3 cups. Thermograms are stored in the computer's memory as well as displayed on the monitor which can be stored on a floppy disks and analyzed later. ΔT is recorded on the Y-scale and temperature of the sample is displayed on the X-axis.

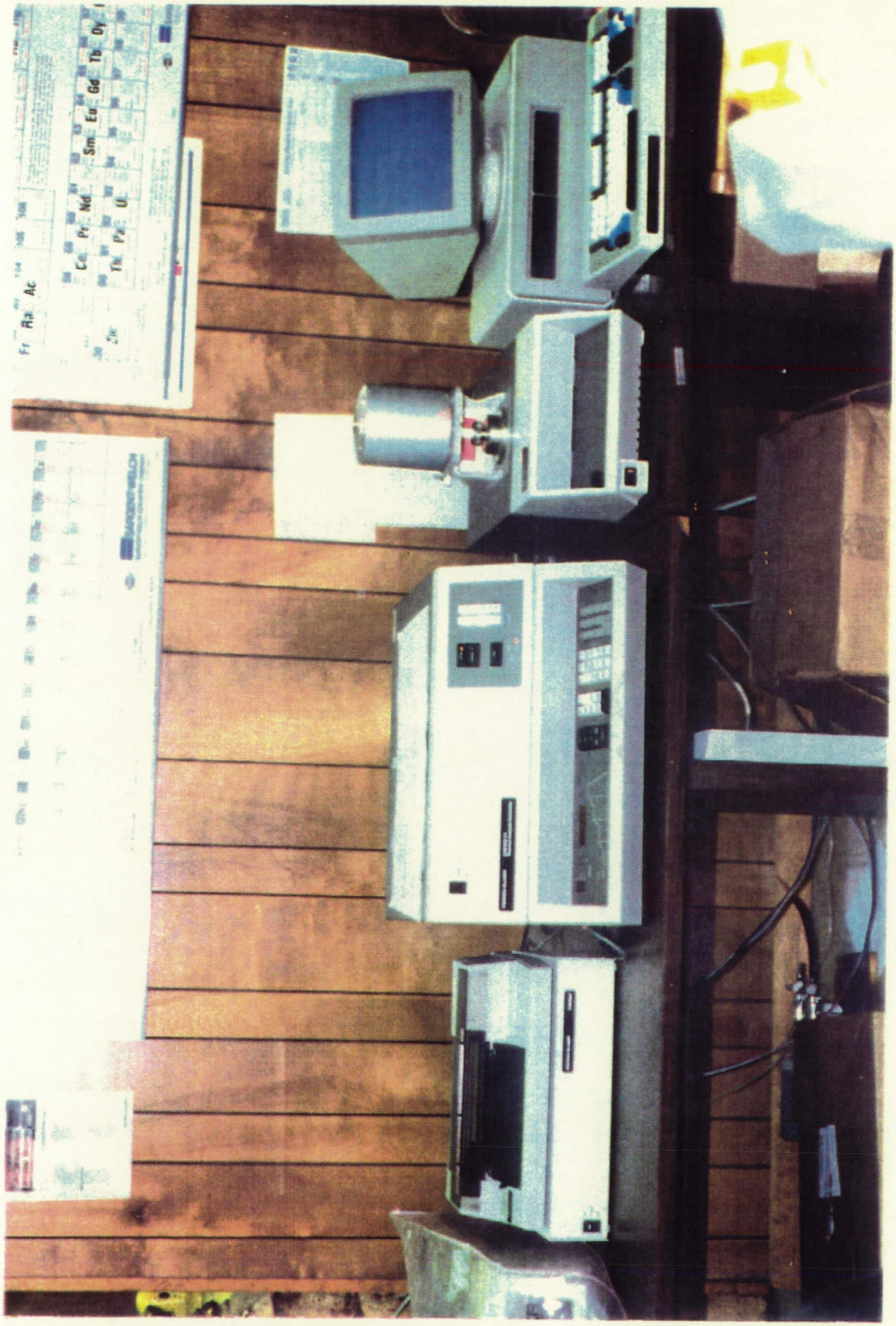

FIG. 20 General View of Perkin Elmer
Differential Thermal Analyzer System DTA 1700

ORIGINAL PAGE
COLOR PHOTOGRAPH

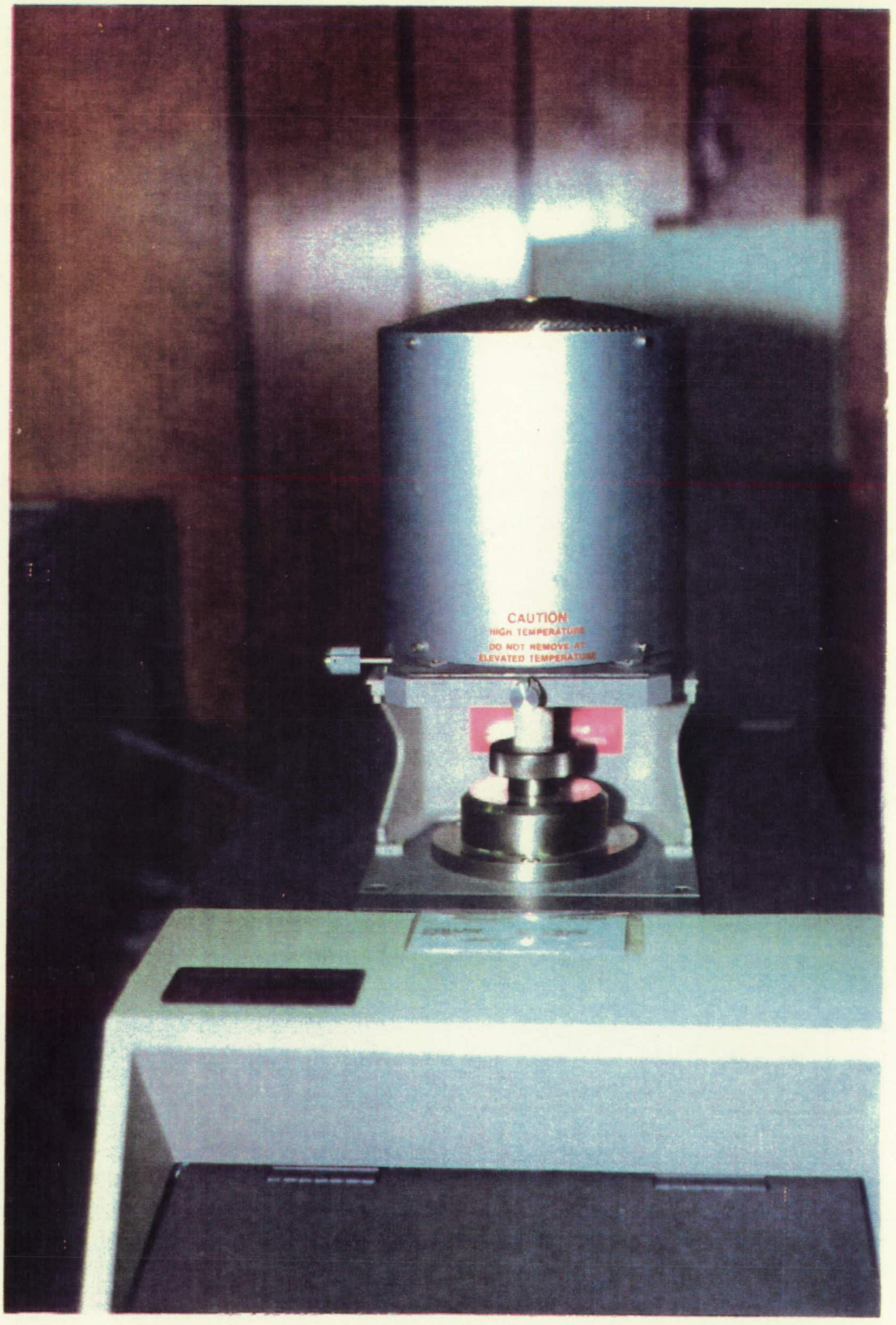

FIG. 21 External View of the Furnace of Differential Thermal Analyzer System DTA 1700

(a) (b)

Fig. 22 (a) DTA Cell with furnace removed (b) Sample and reference curcibles (Alumina crucibles size-6mm^3).

DTA results readily complement those from other methods. For example, γ solvus is traditionally determined metallographically by microscopic examination of quenched samples. Also, carbide reaction is studied by digesting quenched samples and identifying the carbide phase in the extracted residue by means of X-ray diffraction methods.

Differential thermal analysis is not meant as a substitute for metallography or extraction methods but it does offer some distinct advantages. The mass of the sample is smaller than required for a mounted, polished and etched specimen.The time required for DTA is much shorter than other techniques. DTA yields data which is generated by the entire bulk of the sample and is unprejudiced by surface preparation.

One major disadvantage is caused by the small DTA sample size. There is a possibility of unrepresentative data from a single sample due to microsegragation in the material. This, however, can be turned into an advantage in determining homogeneity of the material.

DTA curves of the various samples of MAR-M246(Hf) were recorded in heating as well as cooling cycle in the presence of nitrogen at various program rates. The program heating rate of 15 C/min has been found to yield good results for the superalloy samples.

The differential thermal analysis measurement have also been done on the Ni-based superalloy samples, MAR-M247, Udimet UD-41, Waspaloy, CMSX-2 and CMSX-3 in polycrystalline and single crystal form. These curves are shown in Figs 23 to 38. These superalloys have a nominal percent composition as given in Appendix A. Solidus and liquidus temperatures for all the above alloys have been evaluated from these curves. An approximate method of calculating the solidification range has also been found and the values are found to be in good agreement. The method is outlined in the next section.

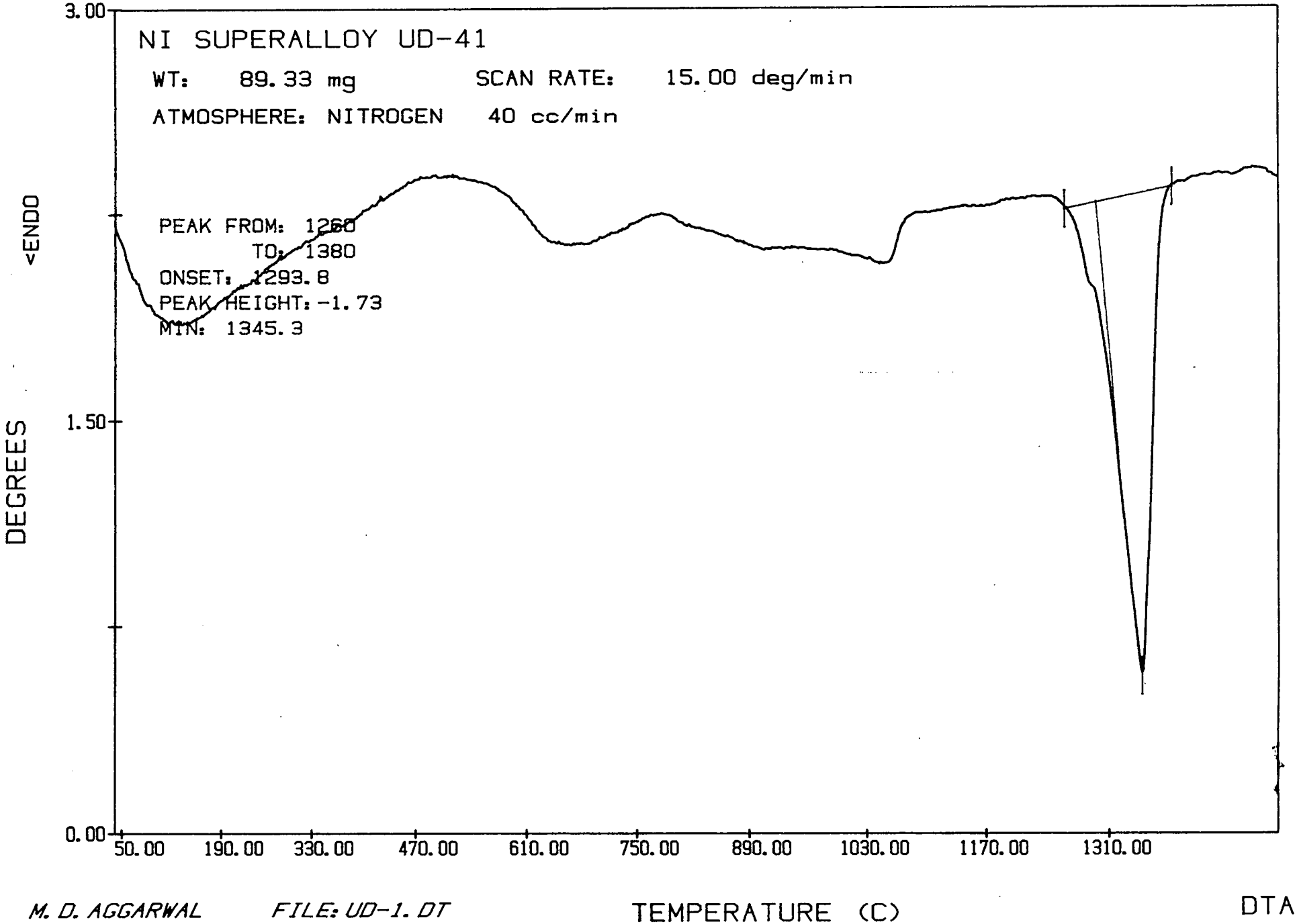
NI SUPERALLOY UD-41
WT: 89.33 mg
SCAN RATE: 15.00 deg/min
ATMOSPHERE: NITROGEN 40 cc/min
PEAK FROM: 1260
TO: 1380
ONSET: 1293.8
PEAK HEIGHT: -1.73
MIN: 1345.3
<ENDO
DEGREES
29
3.00
1.50
0.00
50.00
190.00
330.00
470.00
610.00
750.00
890.00
1030.00
1170.00
1310.00
M. D. AGGARWAL
FILE: UD-1. DT
TEMPERATURE (C)
DTA

Fig.

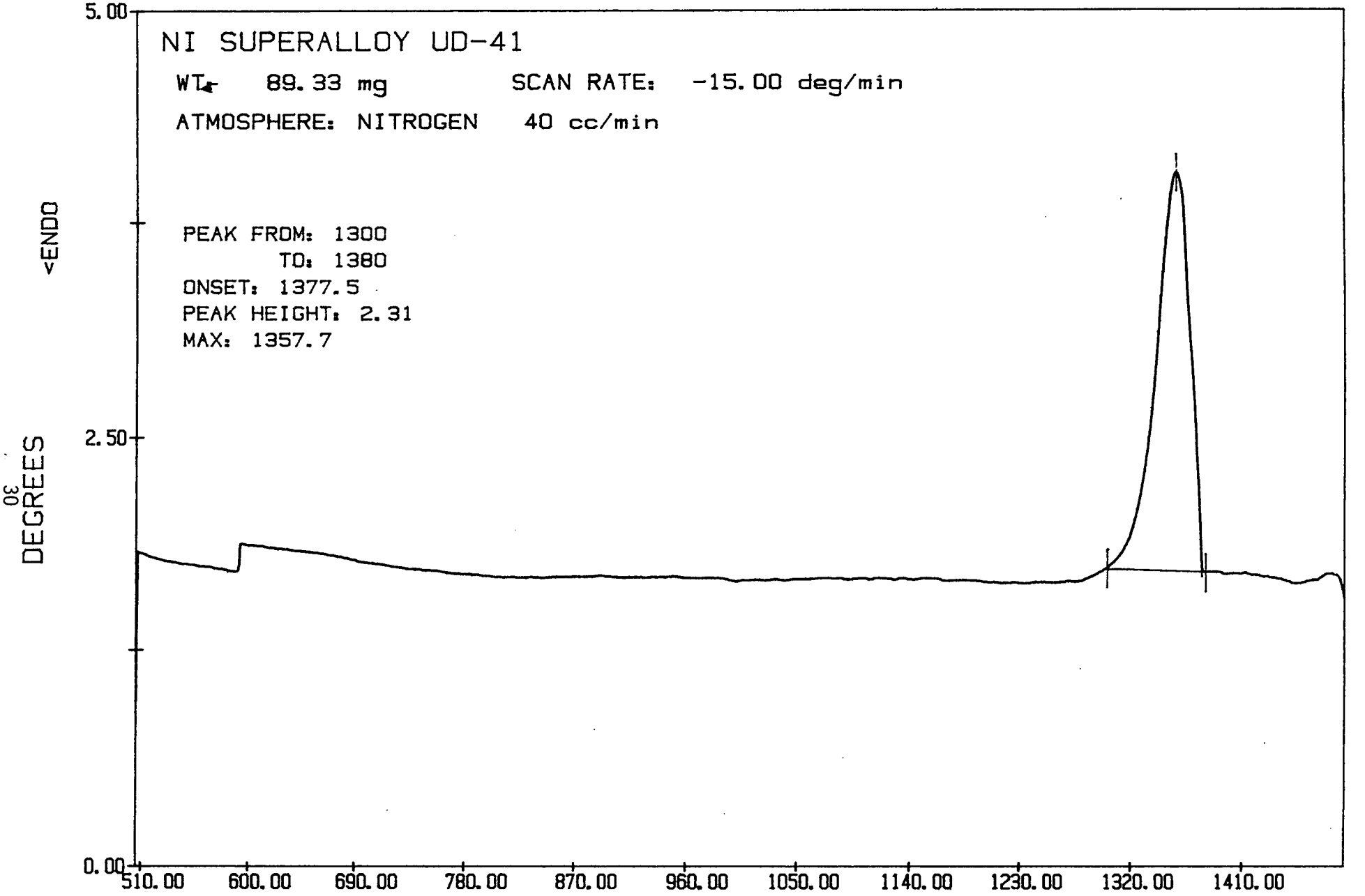

M. D. AGGARWAL *FILE: UD2. DT*

DATE: 88/03/21 TIME: 05: 11

Fig. 24

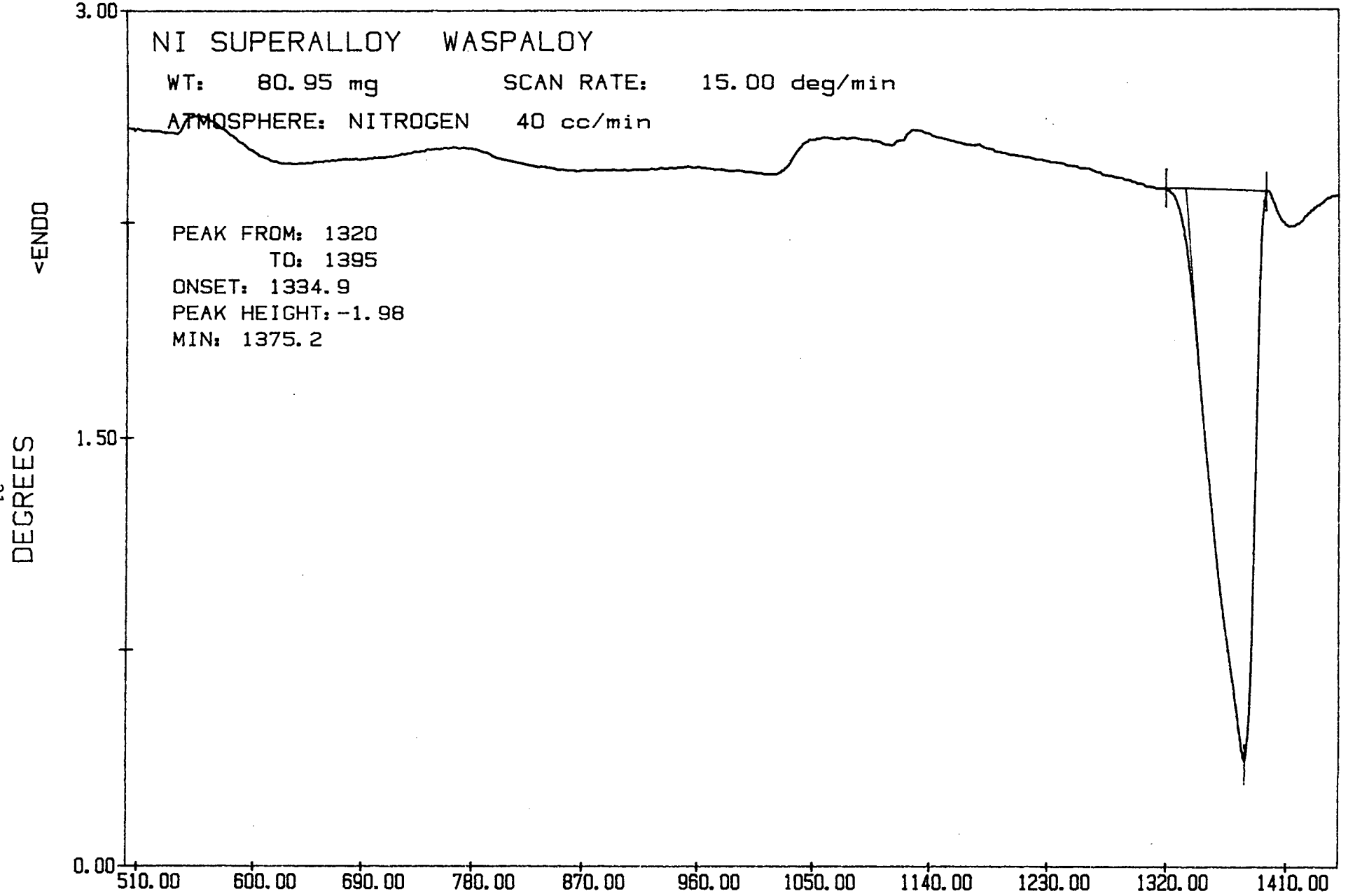

M. D. AGGARWAL *FILE: WA1. DT*

DATE: 88/03/31 TIME: 10:39

Fig. 25

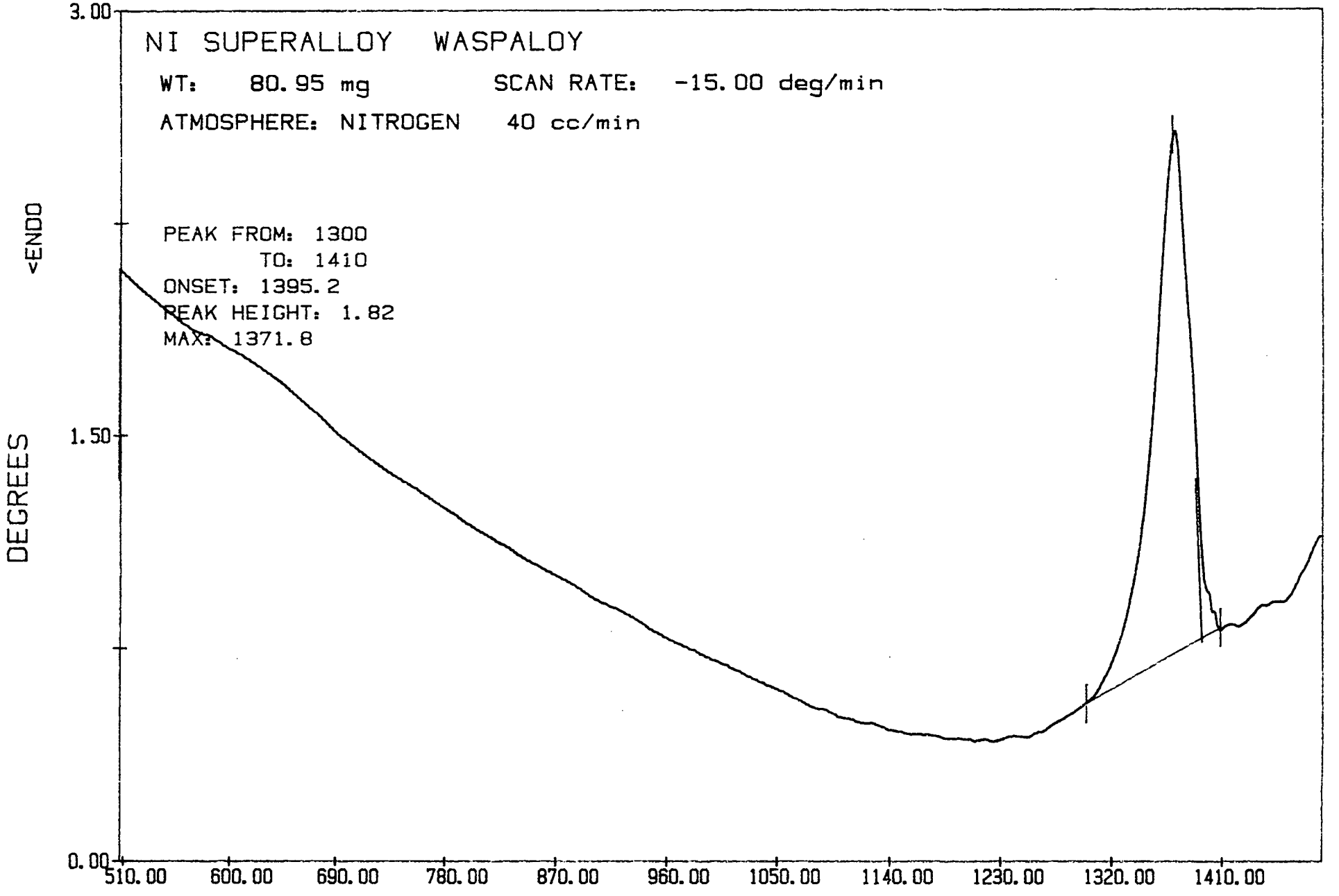

M. D. AGGARWAL *FILE: WAS2. DT*

DATE: 88/03/31 TIME: 12: 17

Fig. 26

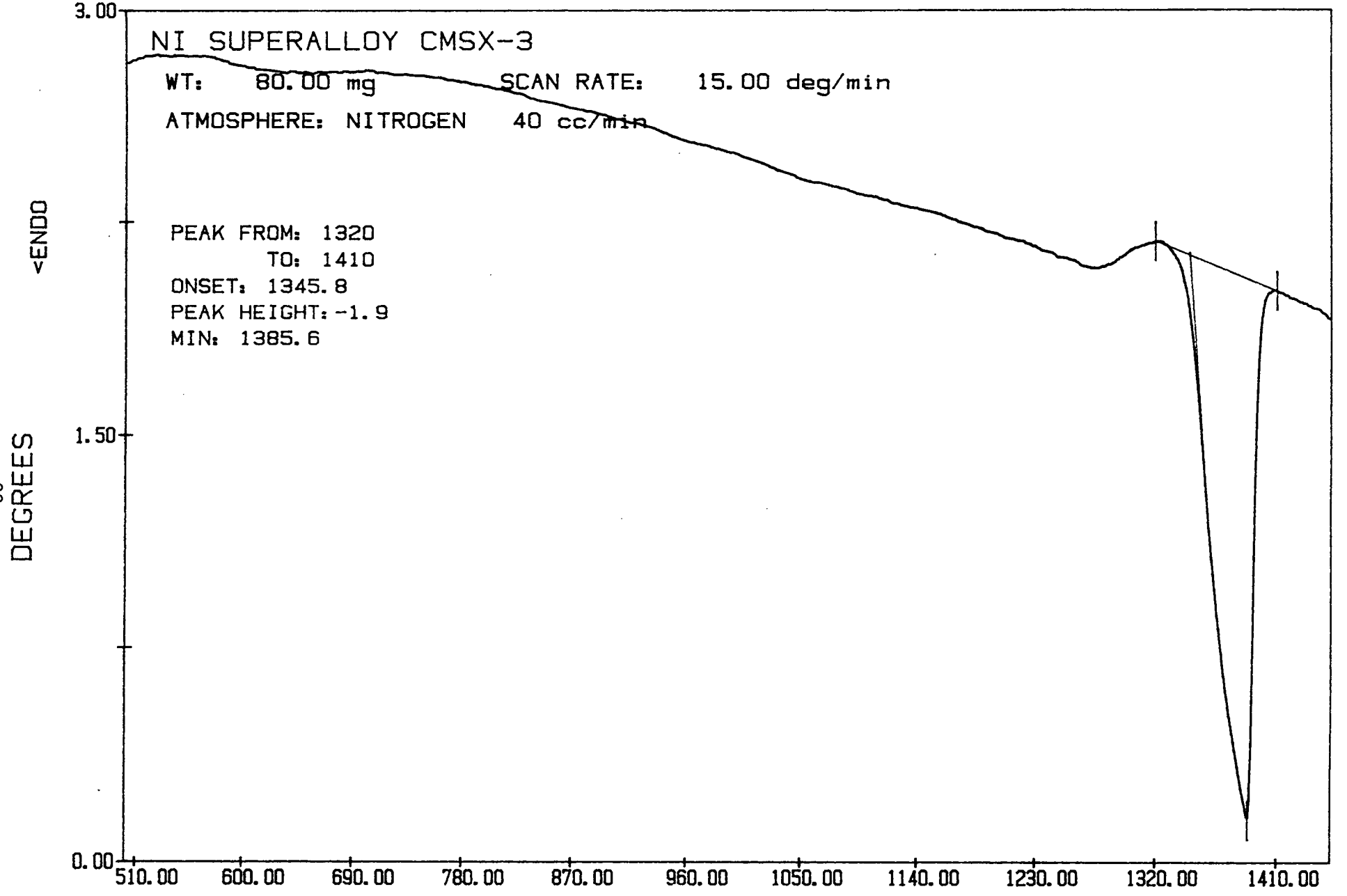

M. D. AGGARWAL *FILE: CM3. DT*

DATE: 88/06/30 TIME: 09: 23

Fig. 27

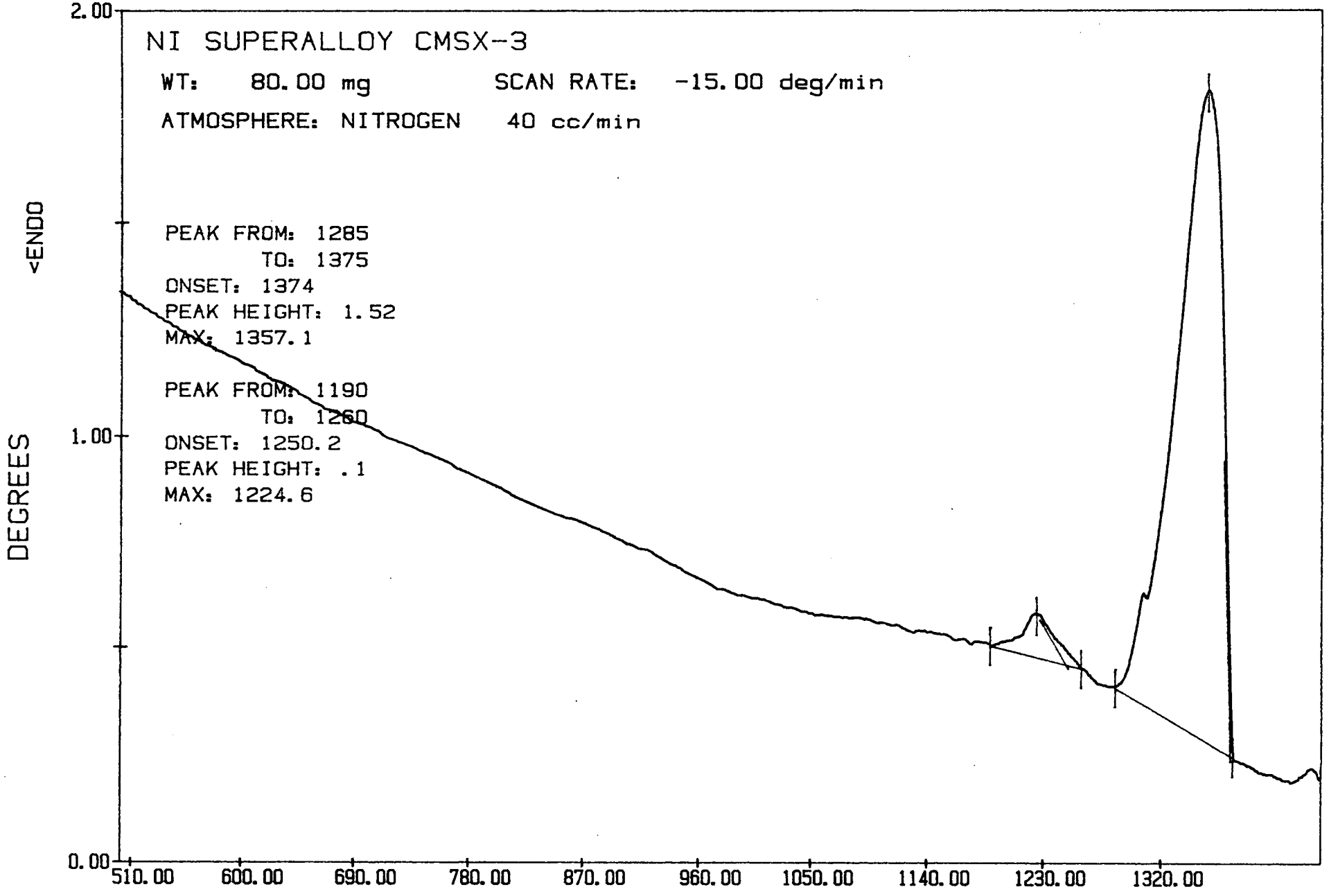

M. D. AGGARWAL *FILE: CM4. DT*

DATE: 88/06/30 TIME: 10:57

Fig. 28

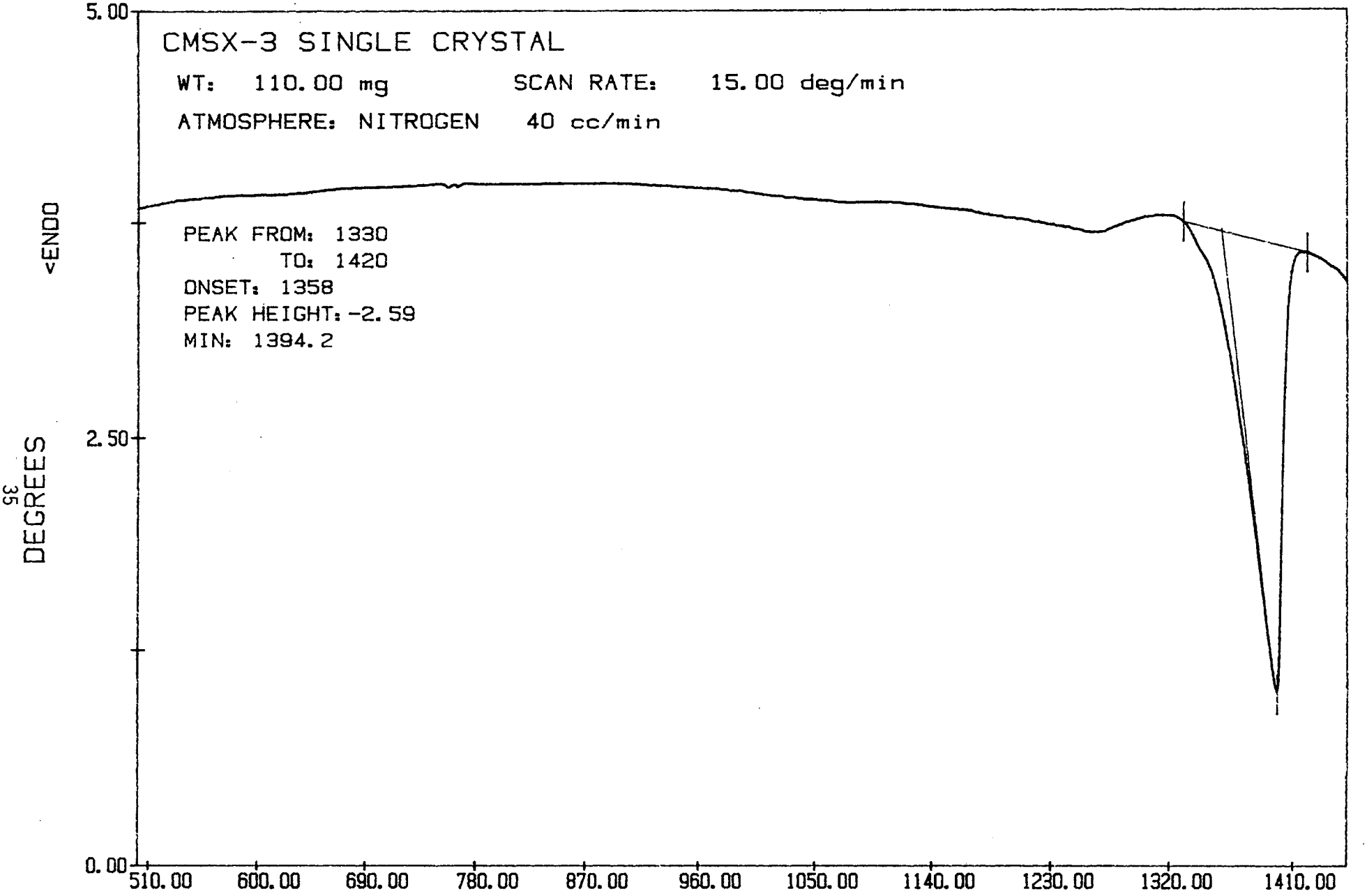

M. D. AGGARWAL *FILE: CM3. DT*

DATE: 88/07/11 TIME: 09: 43

Fig. 29

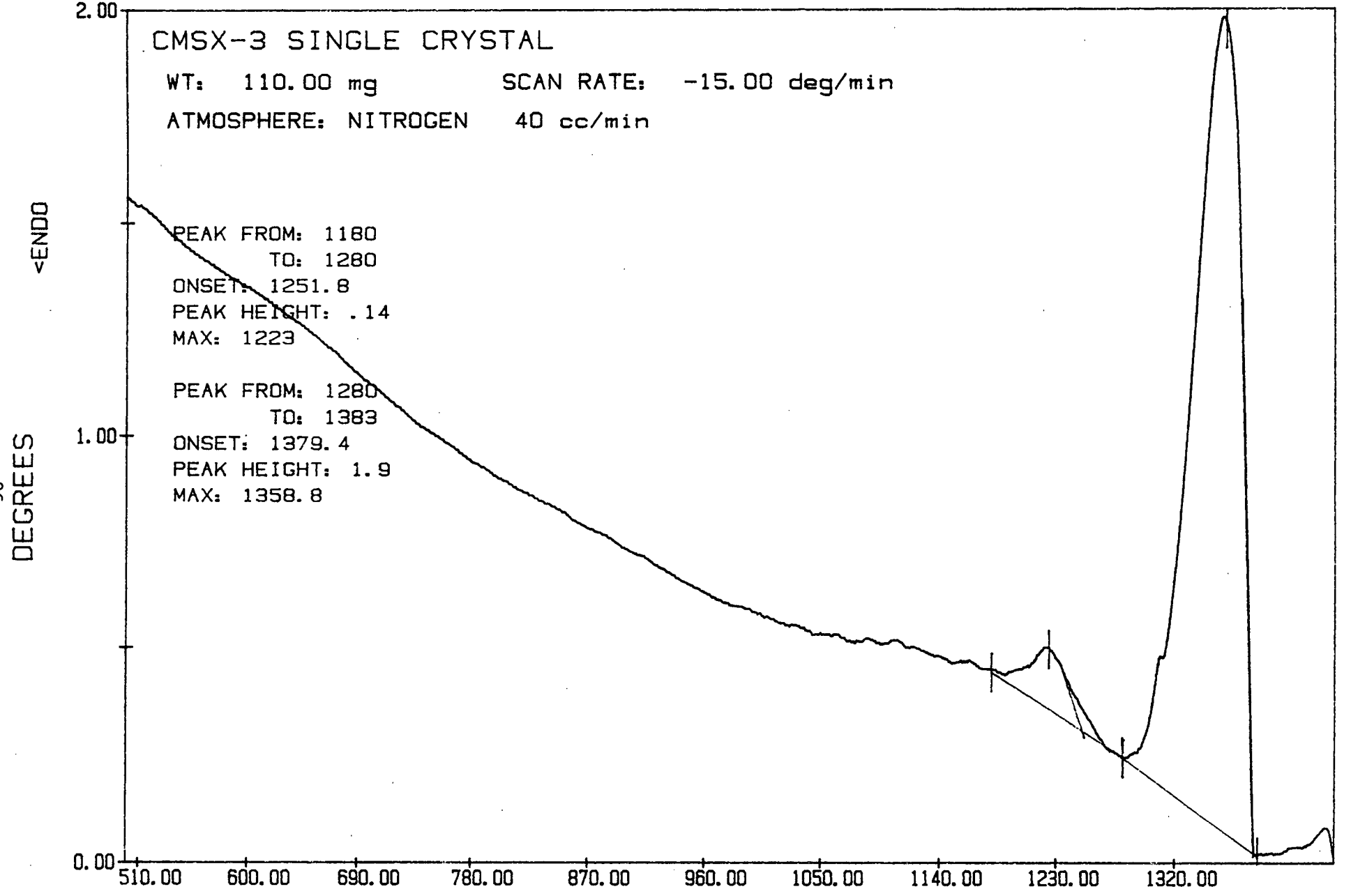

M. D. AGGARWAL *FILE: CM4. DT*

DATE: 88/07/11 TIME: 11:18

Fig. 30

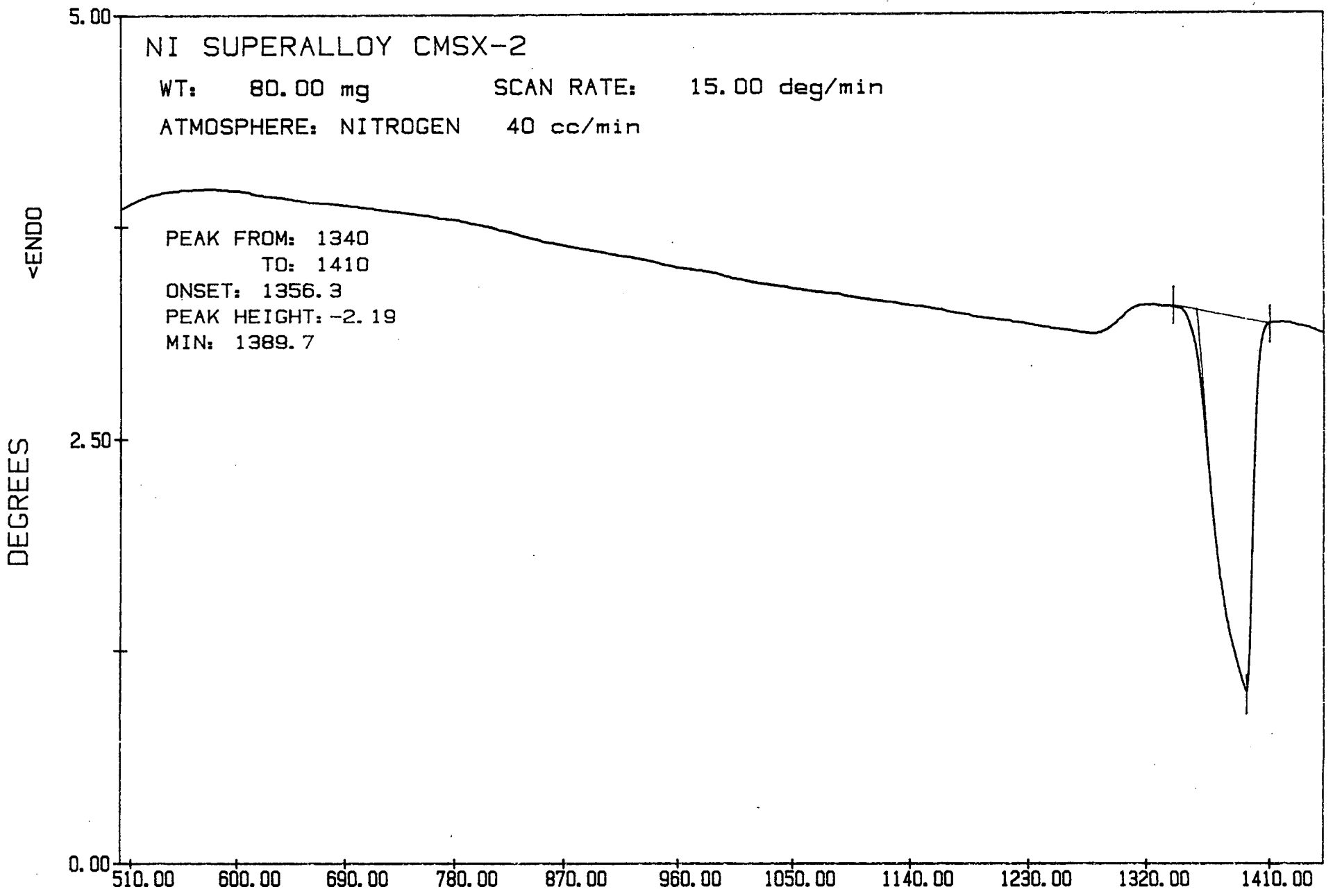

M. D. AGGARWAL *FILE: CM. . DT*

DATE: 88/06/29 TIME: 14:58

Fig. 31

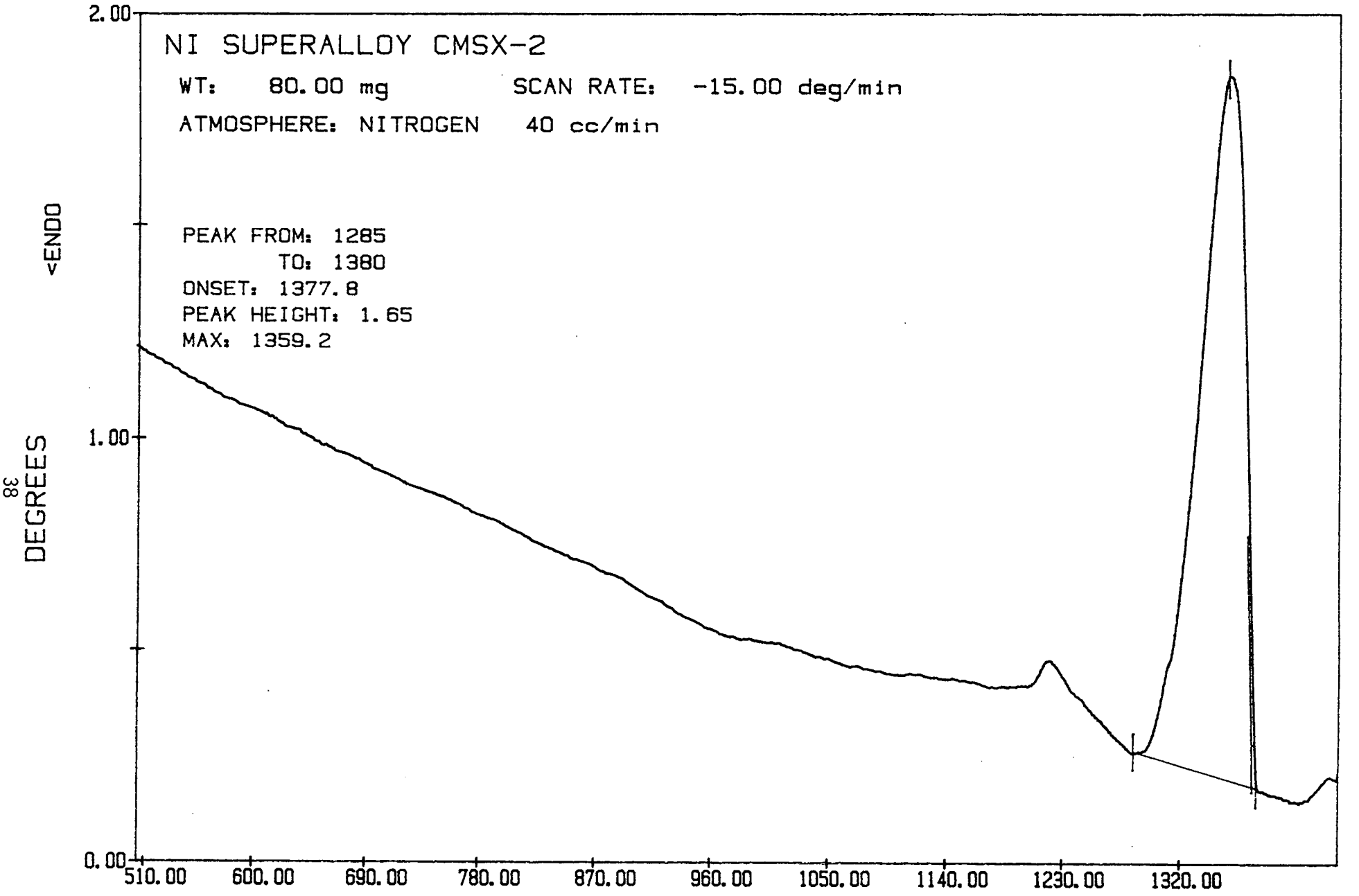

M. D. AGGARWAL *FILE: CM2. DT*

DATE: 88/06/29 TIME: 16:32

Fig. 32

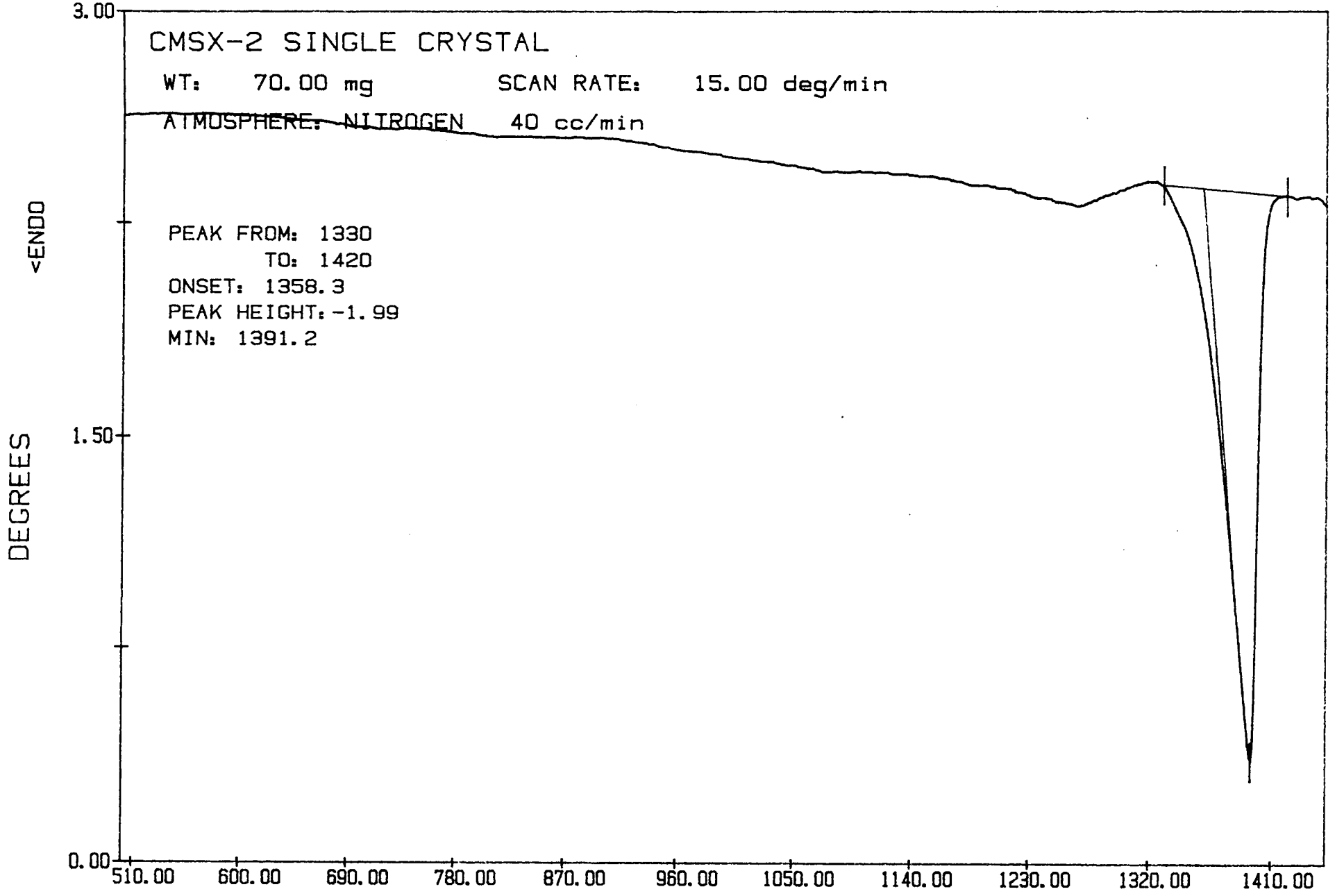

M. D. AGGARWAL *FILE: CMI. DT*

DATE: 88/07/10 TIME: 01:14

Fig. 33

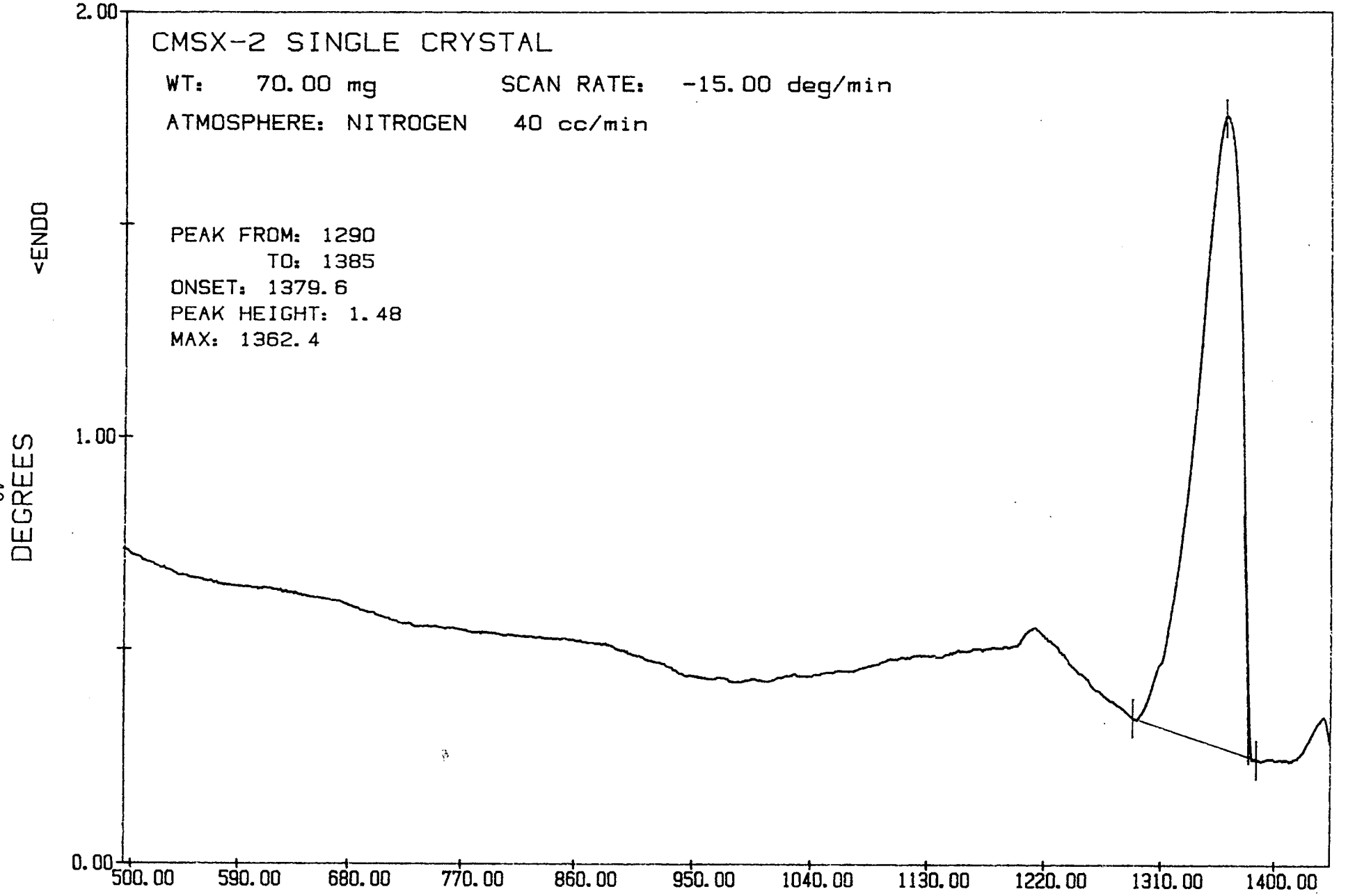

M. D. AGGARWAL *FILE: CM2. DT*

DATE: 88/07/10 TIME: 02: 49

Fig. 34

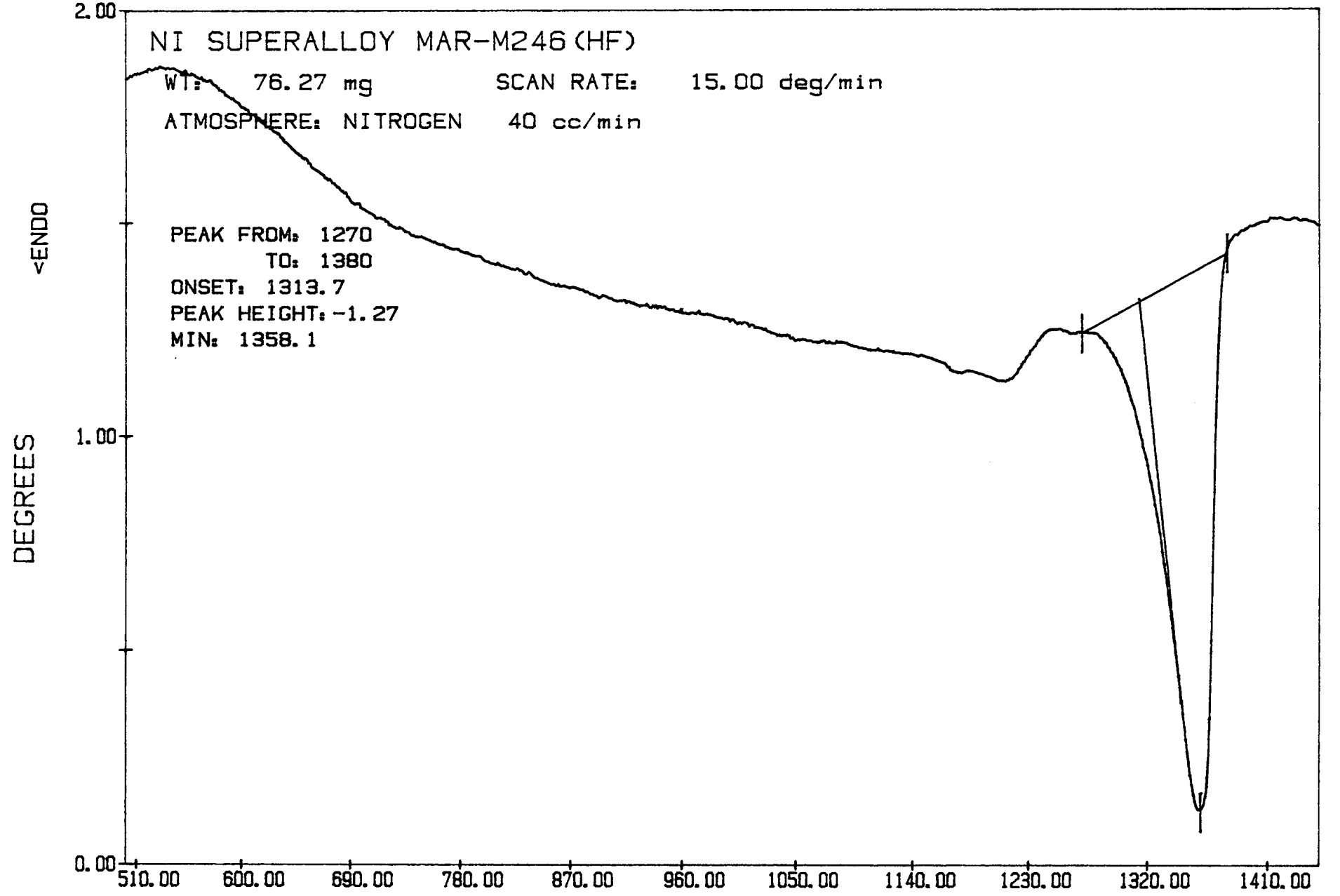

M. D. AGGARWAL *FILE: MAR5. DT*

DATE: 88/03/17 TIME: 09: 28

Fig. 35

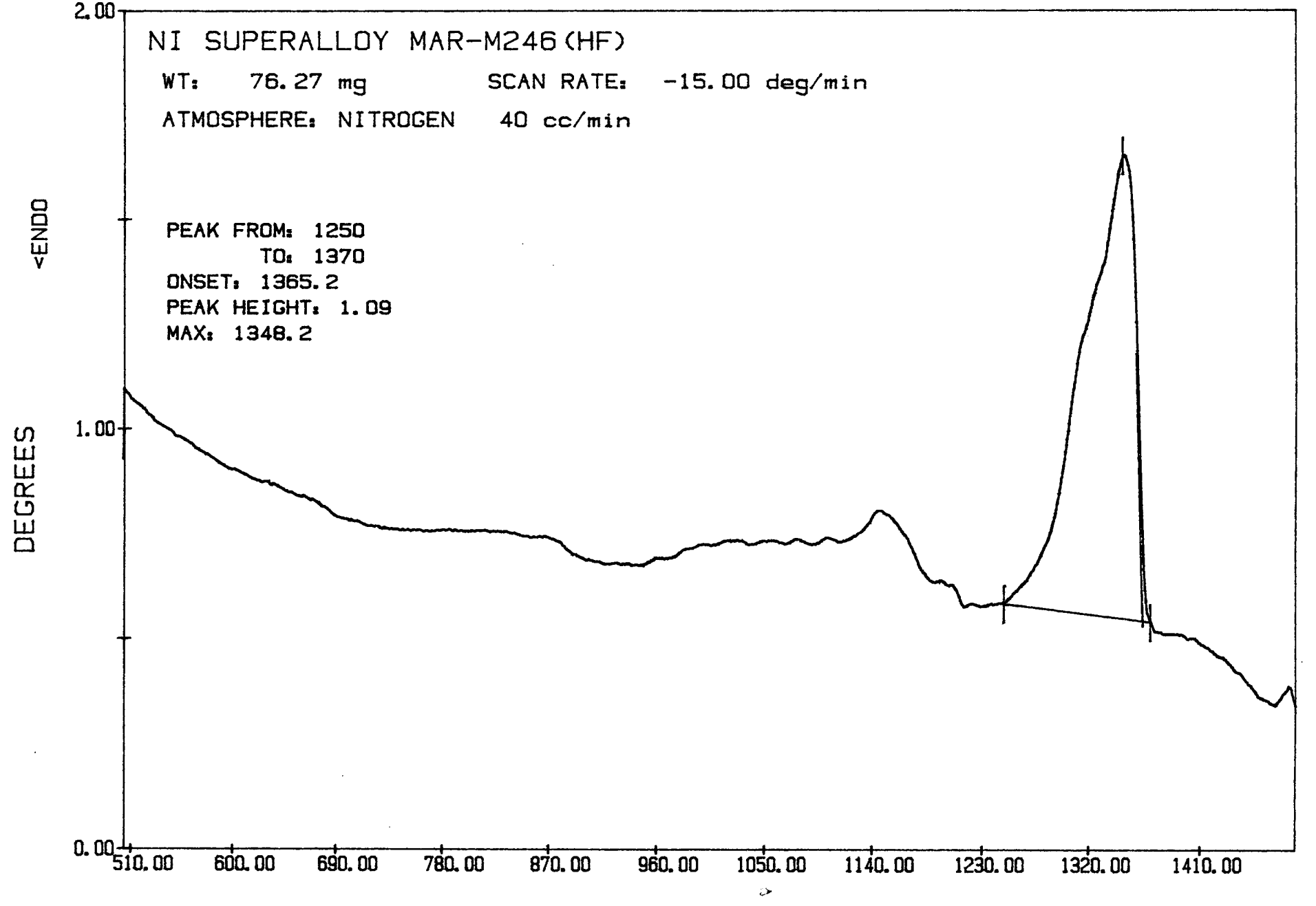

M. D. AGGARWAL *FILE: MAR6. DT*

DATE: 88/03/17 TIME: 11:06

Fig. 36

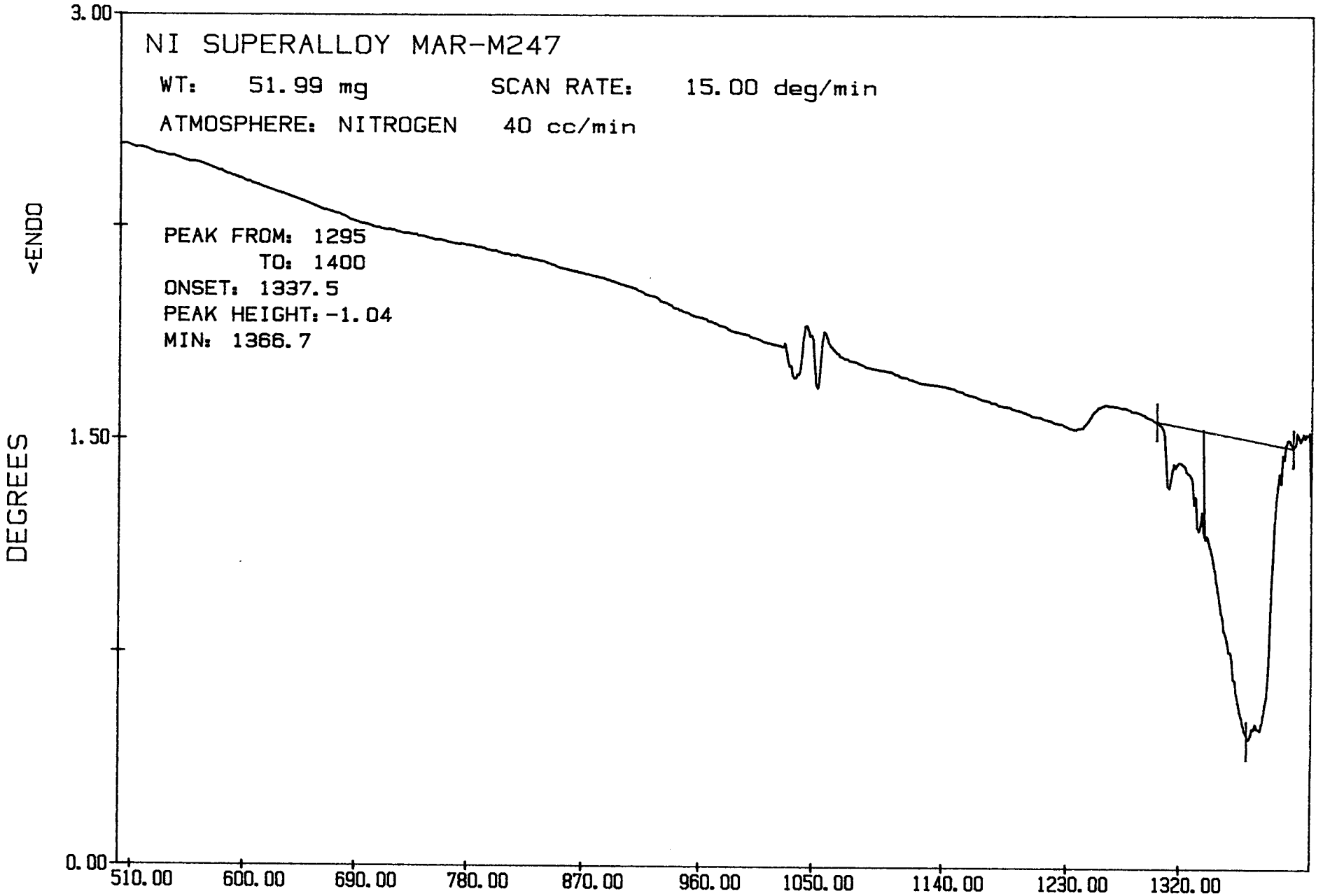

M. D. AGGARWAL *FILE: MA17. DT*

DATE: 88/03/30 TIME: 11:44

Fig. 37

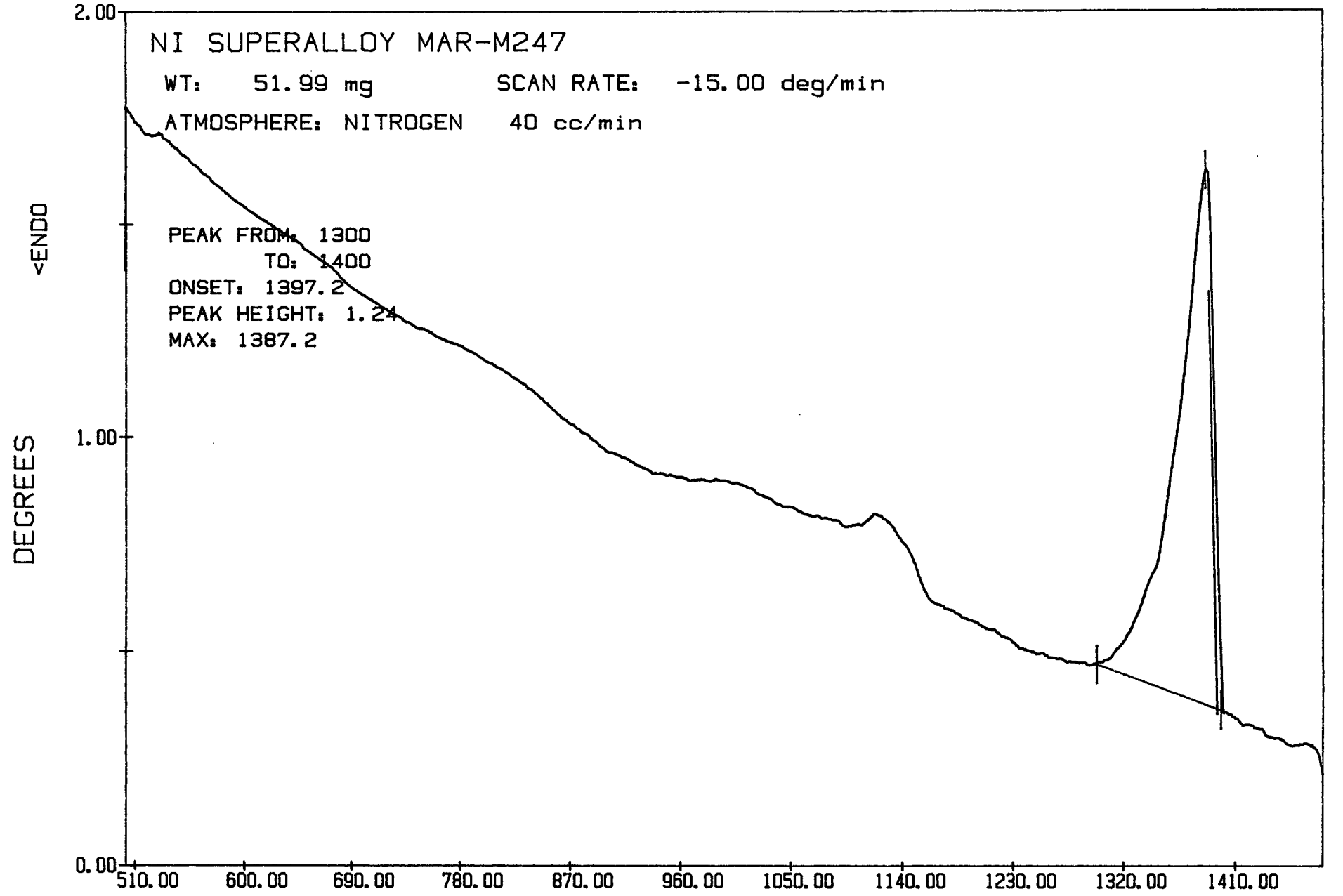

M. D. AGGARWAL *FILE: MA18. DT*

DATE: 88/03/30 TIME: 13:56

Fig. 38

2.5 Approximate method of predicting solidification range of superalloys

For highly diluted solutions, Hayes and Chipman[6] showed that the change in the melting point ΔT of the parent metal M after adding a small amount of component B is given as:

$$\Delta T = \frac{(1-k_{0,b})}{\Delta H_M} N_{L,B} R (T_M)^2$$

where $k_{0,b}$ is the equilibrium distribution coefficient of component B in the parent metal M, ΔH_M is the heat of melting (J/mol) and T_m is the melting point of the metal M (K), $N_{L,B}$ is the molar fraction of component B dissolved in the liquid phase of metal M and R has the usual meaning (8.314 J K^{-1} mol^{-1}).

The equilibrium distribution coefficient $k_{0,b}$ is defined at T=constant by the relationship

$$k_{0,b} = N_{S,B}/N_{L,B}$$

where $N_{S,B}$ is the molar fraction of component B in the solid solution based on metal M.

For highly diluted solutions, as in the case of Ni based superalloys, the liquidus and solidus curves can be replaced by straight lines and the solidification range of the solution M-B,

denoted by $I_B = T_{L,B}-T_{S,B}$ in metal M can be expressed by the relationship

$$I_B=\frac{(1-k_{0,b})}{k_{0,b}}\Delta T=\frac{(1-k_{0,b})^2 T_M^2 R}{k_{0,b}\Delta H_M}N_{L,B}$$

If the parent metal M is represented by Ni, the above equation can be written in the form

$$I_B=832.3\frac{(1-k_{0,b})}{k_{0,b}}\frac{C_B}{M_B}$$

where C_B is the concentration of component B in weight percent, M_B is the molecular mass of component B, I_B is in degrees celcius.

Assuming the mutual independence of the effect of the components on the change of melting point of parent metal M, we can determine the equilibrium solidification range I of the solution

$$I=\Sigma I_B$$

if $k_{0,B}$ and $N_{L,B}$ are known.

This range has been calculated for the Ni-based superalloys MAR-M247, Udimet UD-41, Waspaloy, CMSX-2 and CMSX-3 in polycrystalline and single crystal form and the values compared

with the solidification range evaluated from the differential thermal analysis. The results of calculation for each superalloy are given in Tables 1 to 6.

TABLE 1

Ni-based Superalloy UD-41				
Element	C_B	$k_{0,b}$	M_b	Solidification range
C	0.08	0.22	12.01	15.33
Mn	0.10	0.72	54.94	0.16
Si	0.10	0.36	28.08	3.37
Cr	18.70	0.82	51.99	11.83
Ni	Bal.	1.0	58.70	
Co	10.80	1.03	58.93	0.14
Mo	9.80	0.89	95.94	1.16
Ti	3.21	0.73	47.90	5.57
Al	1.59	0.87	26.98	0.95
Zr	0.07	0.09	91.22	6.20
P	0	0.01	30.97	8.95
Cu	0.01	0.82	63.55	0.01
Ta	0.01	0.74	180.95	0.00
			Total I	53.58

From DTA Curve

T_S = 1293.8 C

T_L = 1345.3 C

Diff. = 52.5 C

TABLE 2

Ni-based Superalloy Waspaloy				
Elements	C_B	$k_{0,b}$	M_b	Solidification Range
C	0.027	0.82	12.01	0.074
Mn	0.03	0.72	54.94	0.049
Si	0.05	0.36	28.08	1.686
Cr	19.19	0.82	51.99	12.14
Ni	Bal	1.0	58.7	
Co	13.1	1.031	58.93	0.172
Fe	0.96	0.94	55.85	0.054
Mo	4.1	0.89	95.94	0.483
W	0.04	1.5	183.85	0.03
Nb	0.04	0.51	92.91	0.168
Ti	3.02	0.73	47.9	5.24
Al	1.31	0.87	26.98	0.785
Zr	0.057	0.086	91.22	5.052
P	0.006	0.006	30.97	26.55
Ta	0.01	0.74	180.95	0.0042
			Total I	52.49

From DTA Curve

T_S = 1334.9 C

Diff. = 40.3 C

T_L = 1375.2 C

TABLE 3

Ni-based Superalloy CMSX-2 (Polycrystalline)				
Elements	C_B	$k_{0,b}$	M_b	Solidification range
Al	5.62	0.87	26.98	3.368
Co	4.6	1.031	58.93	0.061
Cr	7.9	0.82	51.99	4.997
Cu	0.001	0.82	63.55	0.0005
Fe	0.03	0.94	55.85	0.0017
Mo	0.6	0.89	95.94	0.071
Ni	59.729	1.00	58.7	0
Ta	6.0	0.74	180.95	2.52
Ti	1.00	0.73	47.9	1.735
W	7.9	1.5	183.85	5.96
Al+Ti	6.62	0.8	37.44	7.358
			Total I	26.073

From DTA Curve

T_S = 1356.3 C

Diff. = 33.4 C

T_L = 1389.7 C

TABLE 4

Ni-based Superalloy CMSX-3 (Polycrystalline)				
Elements	C_B	$k_{0,b}$	M_b	Solidification Range
Al	5.66	0.87	26.98	3.392
Co	4.6	1.031	58.93	0.061
Cr	7.9	0.82	51.99	4.997
Fe	0.026	0.94	55.85	0.0015
Hf	0.1	0.16	178.49	
Mo	0.6	0.89	95.94	0.071
Ni	59.729	1.00	58.7	0
Ta	6.1	0.74	180.95	2.563
Ti	1.02	0.73	47.9	1.769
W	8.0	1.5	183.85	6.036
Al+Ti	6.68	0.8	37.44	7.425
			Total I	26.315

From DTA Curve

T_S = 1345.8 C

Diff. = 39.8 C

T_L = 1385.6 C

TABLE 5

Ni-based Superalloy CMSX-2 (Single Crystal)				
Elements	C_B	$k_{0,b}$	M_b	Solidification Range
Al	5.59	0.87	26.98	3.35
Co	4.7	1.031	58.93	0.0618
Cr	7.9	0.82	51.99	4.997
Fe	0.032	0.94	55.85	0.0018
Mo	0.6	0.89	95.94	0.071
Ni	59.728	1.00	58.7	0
Ta	6.0	0.74	180.95	2.52
Ti	0.98	0.73	47.9	1.70
W	7.9	1.5	183.85	5.96
Al+Ti	6.57	0.8	37.44	7.303
			Total I	25.966

From DTA Curve

T_S = 1358.3 C

T_L = 1391.2 C

Diff. = 32.9 C

TABLE 6

Ni-based Superalloy CMSX-3 (Single Crystal)				
Elements	C_B	$k_{0,b}$	M_b	Solidification Range
Al	5.6	0.87	26.98	3.356
Co	4.6	1.031	58.93	0.061
Cr	7.8	0.82	51.99	4.933
Fe	0.026	0.94	55.85	0.0015
Hf	0.1	0.16	178.49	
Mo	0.6	0.89	95.94	0.071
Ni	59.794	1.00	58.7	0
Ta	6.0	0.74	180.95	2.52
Ti	0.99	0.73	47.9	1.72
W	7.9	1.5	183.85	5.961
Al+Ti	6.59	0.8	37.44	7.325
			Total I	25.947

From DTA Curve

T_S = 1358 C

Diff. = 36.2 C

T_L = 1394.2 C

3. Publications / Presentations & reports relating to this project

1. Solidification range of Ni-based superalloy MAR-M246(Hf) J.Ala Acad. Science 59(1958) 152.

2. "Microstructural characteristics of Ni-based superalloy at high temperatures" presented at NASA/HBCU forum at Atlanta University center during 25-28, 1987

3. Differential thermal Analysis and heat treatment of Ni-based superalloy presented at Alabama University during Oct 11-13,1988.

4. A study of microstructural characteristics and differential thermal analysis of Ni-based superalloy" proceeding of NASA-HBCU space and engineering forum held at Alabama A&M university, Huntsville, Al during March 22-23,1989 pp382-389.

5. Semi-Annual Technical Report AAMU-NAG-001 submitted to NASA/MSFC May,1987.

6. Second Year Semi-Annual Technical Report AAMU-NAG-002 submitted to NASA/MSFC September,1988.

REFERENCES

1. C.T.Sims, N.S.Stoloff and W.C.Hagel Eds. **Superalloys** (John Wiley, New York, 1987).

2. G.F. Vander Voort Ed. **Applied Metallography** (Van Nostrand Reinhold, New York, 1986).

3. G.Blann, **Metallography 17**,89(1985).

4. F.N.Rhines, **Microstructology** (Riederer-Verlag, Stuttgart, 1986).

5. W.W. Wendlandt,**Thermal Analysis** (John Wiley, New York,1986).

6. A. Hayes and J.Chipman, Trans. AIME **135**,85 (1939).

APPENDIX A

Composition of Ni-based Superalloy MAR-M246(Hf)

Elements	Weight % Composition	Melting Point (C)	Solubility in Ni (wt%)
Ni	58.035	1453	
Co	10.0	1495	complete
W	10.0	3410	40
Cr	9	1857	47
Al	5.5	660	11
Mo	2.5	2617	37.5
Hf	1.75	2227	
Ti	1.5	1660	12.5
Ta	1.5	2996	36
C	0.15	3367	0.55
Zr	0.015	1852	
B	0.015	2079	

Weight percent composition of various elements in Nickel for superalloys MAR-M247, UD-41 and Waspaloy

Elements	MAR-M247 Sample #717816 (Wt %)	UD-41 #88292 (Wt %)	Waspaloy #911971 (Wt %)
C	0.139	0.08	0.027
Mn	0.03	<0.10	0.03
Si	0.03	<0.10	0.05
Cr	8.29	18.70	19.19
Ni	60.0365	53.364	58.023
Co	9.93	10.80	13.10
Fe	0.09	0.20	0.96
Mo	0.70	9.80	4.10
W	9.91	-	0.04
Nb	0.01		0.04
Ti	1.00	3.21	3.02
Al	5.48	1.59	1.31
B	0.013	0.004	0.005
Zr	0.04	<0.07	0.057
S	0.0005	0.002	0.002
P	0.001	0.002	0.006
Cu	0.01	0.012	0.02
Ta	3.02	0.01	0.01
Hf	1.27	0.03	0.01

Weight percent composition of various elements in Nickel for polycrystalline superalloys CMSX-2 and CMSX-3

Elements	CMSX-2 (Polycrystalline) Weight %	CMSX-3 (Polycrystalline) Weight %
Al	5.62	5.66
Co	4.6	4.6
Cr	7.9	7.9
Cu	0.001	
Fe	0.03	0.026
Hf	-	0.1
Mo	0.6	0.1
Ni	59.729	59.314
Ta	6.0	6.1
Ti	1.0	1.02
W	7.9	8.0
Al+Ti	6.62	6.68

Weight percent composition of various elements in Nickel for single crystal superalloy CMSX-2 and CMSX-3

Elements	CMSX-2 (Single crystal) Weight %	CMSX-3 (Single crystal) Weight %
AL	5.59	5.6
Co	4.7	4.6
Cr	7.9	7.8
Fe	0.032	0.026
Hf	-	0.1
Mo	0.6	0.6
Ni	59.728	59.794
Ta	6.0	6.0
Ti	0.98	0.99
W	7.9	7.9
Al+Ti	6.57	6.59